CHALMERS

Multibody modeling and vibration dynamics analysis of washing machines

Thomas Nygårds · Viktor Berbyuk

Abstract

In this paper a computational model of a horizontal axis washing machine is presented. The model has been built using a theoretical-experimental methodology consisting of integration of multibody system (MBS) formalism, detailed modeling of machine functional components and experimental data based validation. The complete model of a washing machine is implemented in the commercial MBS environment Adams/View from MSC.Software.

An undesirable impact of washing machine operation on the surroundings is vibration and noise. The impact comes from system dynamics and poorly distributed load inside the drum, creating an imbalance. To get insight into vibration dynamics extensive simulations have been performed for washing machines in service as well as for machines in the developing stage by using the created computational model.

This paper presents several results of numerical studies of the vibration dynamics of washing machines including the study of sensitivity of system dynamics with respect to suspension structural parameters, and the results of investigation of the potential of the automatic counterbalancing technology for vibration output reduction. In particular, simulations of the considered two plane balancing device has shown an existing significant potential in eliminating unbalanced load at supercritical spinning speed, resulting in a substantial vibration reduction in washing machines.

Commemorative Contribution.

T. Nygårds · V. Berbyuk

Department of Applied Mechanics, Chalmers University of Technology, Göteborg, Sweden

e-mail: thomas.nygards@gmail.com, viktor.berbyuk@chalmers.se

1 Introduction

A washing machine is a complex multibody mechatronic system where valves, pumps, heaters and motors are controlled with integrated controllers based on sensor information such as water levels, temperatures, load inertia, and tub motion. The structure of a washing machine usually comprises several highly nonlinear components such as friction dampers, rubber feet, rubber bushings, and other. Modeling and analysis of dynamics of a washing machine is a great challenge. The research focus currently directed towards topics like energy efficiency, washing and spinning performance, water consumption, and noise. One traditional and still very much relevant issue is stability of washing machines called “walking”. All of the above issues are strongly coupled to system vibration dynamics. Studies of washing machine dynamics, control and optimization problems are not as commonly reported in literatures as done other systems, even if there have been much applied work done. In [1] several models of suspension less washing machines are considered with the focus of modeling and compared on conceptual levels. The topic of the paper is walking of washing machines and it is treated with the establishment of design criterias to be fulfilled at static conditions. Several comparisons of vertical and horizontal axis washing machines are presented in [2]. Top and bottom and cross mount suspension systems are modeled in the plane and compared. Also the topic of automatic (passive) counterbalancing is treated and concepts for dealing with this problem are discussed. The paper [3] presents a simplified 3D dynamic model of a horizontal-axis portable washing machine with a balancing device. Also different criteria for determination of the margin to walking during the spinning cycle are presented, extending [1]. In [4] the focus is put on prediction of the tub motion together with stability issues of vertical and lateral motion of the housing. In [5] the dynamic analysis of a drum-type washing machine has been conducted using a simplified dynamic model considering gyroscopic effects. Its mathematical model has 12 degree of freedom and models flexibility the drum and bearings with a discretized approach. Dynamic analysis is performed using Matlab. For the purpose of numerical verification, the results for unbalance response are presented and compared with the experimental vibration test. The housing is not taken into consideration.

Computational power development under recent years has enabled the use of modeling tools like in [6] where the software Dymola/Modelica is used with focus towards motor control. Commercial multibody software which reduces the step from CAD environment to a dynamic model has have become available and several models constructed in this type of environment

have been developed, [7]. For example in [8] a rigid body model is constructed and in [9] a rigid body model of the drum-tub system implemented in MSC.Software/Adams is completed with flexible components of the housing and used with good prediction results for feet forces.

One promising technology for vibration reduction is counterbalancing. Several strategies to counterbalance an imbalanced load have been proposed. Some are active solutions which require external sensing and control to position counteracting solid masses. Simulations on such devices have been performed in one plane in [3] and two planes [10]. Other solutions to remove static imbalance involve translation of the spinning axis relative to the drum [11-13] by using different mechanisms to control its eccentricity. Using water, which is easily accessible in washing machines, to actively position the total center of mass has also been discussed and studied in [11]. There are also passive solutions to the problem of counterbalancing. In a passive solution no external control stimuli to position the counterweights is needed, instead the positioning is done with the circulatory forces coming from rotation of a counterweight. Passive counterbalancing can be done with a liquid filled ring called the Leblanc balancer. In [14] a mathematical model of such a hydraulic balancer in steady state condition was derived and implemented in a model of a vertical axis washing machine dynamic analysis of an automatic washing machine during spin drying mode. A mathematical model of the hydraulic balancer at steady state is validated by the experimental result of the centrifugal force. Experiments were performed on a washing machine during spin drying mode, and data were compared with the simulation results. The technology is also discussed in [2]. In [15] a similar derivation of the technology is presented. Passive balancing, also called automatic balancing can also be done with solid masses like in [2] where a concept based on an elastically suspended solid ring which can move in the cross axis plane radially is presented. But typically, the masses consist of balls of stainless steel [16, 17, 18] or with pendulums or sliders like in [19].

In this paper the dynamics of a washing machine during spin-drying of the clothes is of special interest. Spin-drying, also called spinning, starts at the speed at which the clothes *start* to stick to the drum of the machine. The speed can be calculated according to (1), where the force affecting a body with mass m rotating in a circular trajectory with radius r at constant speed $\omega=2\pi f_{\text{stick}}$ equals the gravitational force mg.

$$mr\omega^2 = mg \Rightarrow$$
$$f_{stick} = \frac{1}{2\pi}\sqrt{\frac{g}{r}} \tag{1}$$

In household washing machines with diameter of about 30 to 50 cm the sticking will occur at 1.3 to 1 Hz (80 to 60 rpm). The speed at which the clothes stop to tumble around completely is higher, as (1) is valid for the condition when the load is at the angular position corresponding to the top of the drum.

The purpose of this paper is to present a MBS model of a commercial frontloaded washing machine built for analysis of spinning related performance. The model has been built using a theoretical-experimental methodology with which experimentally validated models of functional components have been incorporated into a computational multibody systems model. The computational model has been implemented in Adams to enable use with an Adams-Matlab interface for clustered simulation and optimization. The methodology and model is developed to enable the study of vibration attenuation strategies and for structural optimization of washing machines to improve their vibration performance.

To study the dynamics of the washing machine both experimental and theoretical tools are used. Several test-rigs have been developed for measurements on the complete system as well as for measurements on individual components of the washing machine. The main theoretical tool consists of a model built from several sub models of the key components of the system which are put together. The components are so called functional components (FCs) which together with constraints and kinematic excitation form the complete washing machine. The strategy for modeling is well suited to be combined with component measurements. It was selected to comply with the overall goal of the project in which this work has been performed, being development of tools for improvement of the performance of washing machines. With a model which can be broken down to sub models, sensitivity analysis and optimization of components are facilitated, due to the strong coupling between the sub model and the physical components.

The paper is organized as follows. In section 2 the mechanical model of a washing machine is described with focus on all types of system functional components and constraints between them. Section 3 outlines the developed computational model of a generic horizontal axis washing machine by using commercial multibody system software Adams from MSC.Software. Detailed mathematical models of system functional components are presented. Descriptions of the several developed test rigs and results of components parameters identification, validation of models and experimental study of washing machine vibration dynamics are presented in section 4. Applications of the developed theoretical-experimental methodology to analysis of vibration dynamics including the study of active balancing of washing machine are found in section 5. Finally, a summary of the main

contributions of the paper and outlook of the future research are given in section 6, conclusions.

2 Mechanical model

A modern washing machine as considered in the topic of this paper is a controlled multibody system comprising a rotor, or drum, suspended to a water container/tub with bearings in one or both ends. Water and detergent are added to the tub for the washing cycle. When the drum rotates a flow of water and detergent is created which cleans the load. The rotary motion of the drum also used after the washing to create a flow of water through the load during rinsing and for water extraction during spin drying cycle. The tub is in its turn suspended inside a housing using a relatively soft suspension system. The suspension system is designed to limit the propagation of vibrations from the tub to the housing and further on out into the floor structure of the surroundings where the machine is placed. The suspension is also needed to prevent the machine from moving out of its installation position during spinning. This undesired behavior is called walking and can be a problem mostly for consumer machines which seldom are fixed to the floor when installed. If the machine is placed on a surface which has a sufficiently coarse structure providing high enough friction, the problem is low as the machines nowadays have imbalance limiting hardware and software. So, the problem of the machines jumping around is smaller, but given bad installation conditions washing machines might still walk.

In this paper the machine which has been the focus of modeling comprises a bottom mount suspension system. The suspension consists of four struts, each with a spring and a friction damper integrated into one unit. Each strut is placed between the corner of the bottom plate of the housing and the tub. At the end connection points rubber bushings are placed. At the lower connection point there is a round symmetric bushing of 60^o shore, at the upper connection a squared bushing is mounted inside a steel cup. This bushing is made of 55^o shore rubber. To provide adjustment to uneven floors the machine has four hard rubber feet of 80^o shore, one in each corner of the machine. The rubber is fastened to a screw which together with threads in the bottom plate enables height adjustment.

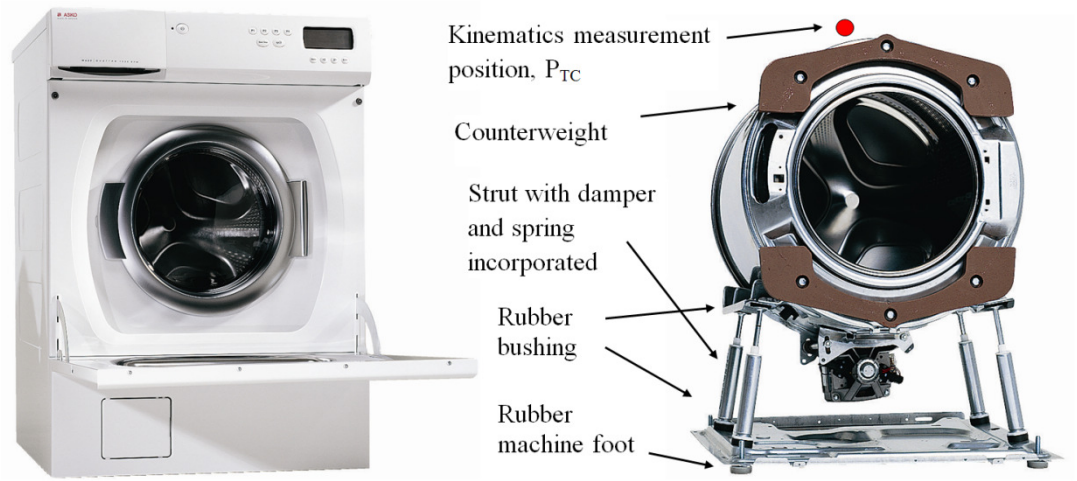

Fig. 1 The studied washing machine and its internal structural parts

One feature of the machine which reduces the modeling complexity a lot is design of the door seal. In most machines the front door is hinged to the housing on one side and locked closed on the other side. To seal the gap between the vibrating tub and the still standing door a large rubber bellow is most commonly used. It can be a problem to model this bellow correctly if it is stiff and/ or its shape makes it influence on the movement of the tub. Normally it is approximated with a multidimensional spring-damper like in [1]. In the machine modeled in this paper the door is fixed to the moving tub. This enables the use of an ordinary rubber seal/gasket. As a result, in the model, the whole door-seal-tub system can be merged with the rest of the tub parts into one body.

It is assumed that the mechanical system modeling the washing machine comprises a set of inertial functional components (IFCs), stiffness functional components (SFCs), damping functional components (DFCs), and stiffness-damping functional components (SDFCs). All the functional components are joined by couplings derived from the physical washing machine design.

To the group of IFCs belong all parts of the washing machine which exhibit inertia properties. In our consideration these are: the drum, the tub, the unbalanced load, the housing (outer casing), the motor rotor, the suspension strut pistons, and the suspension strut cylinders (see Fig. 2).

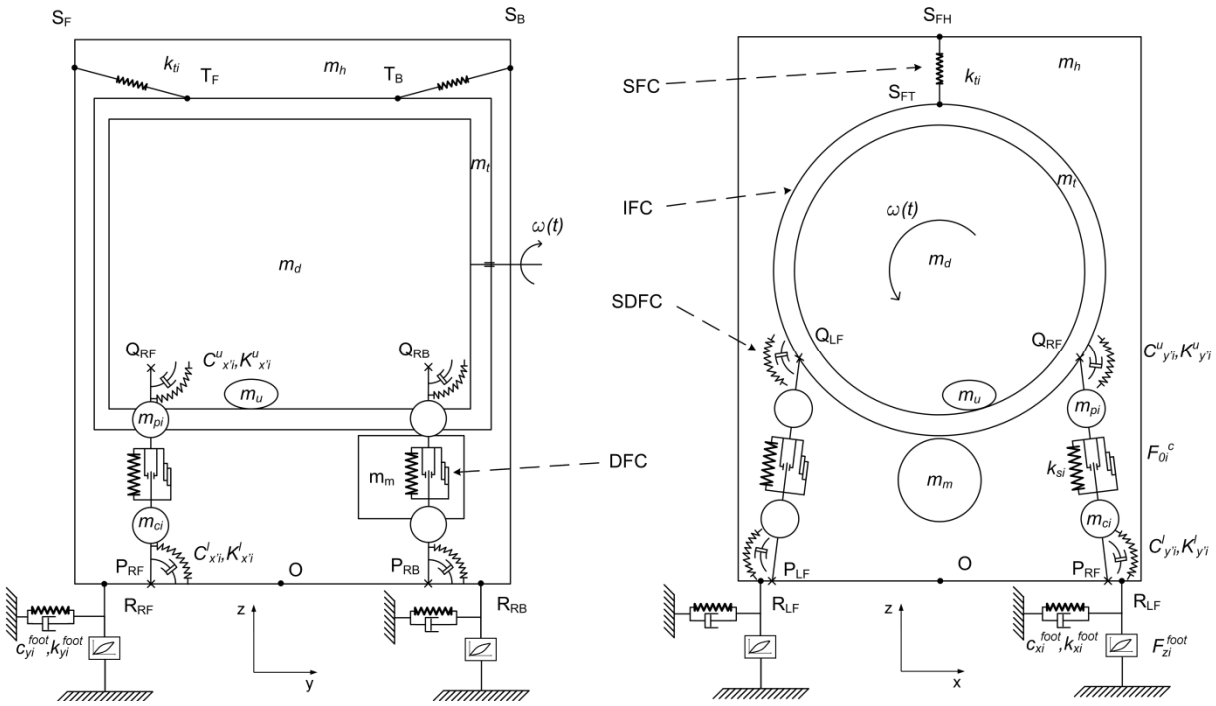

Fig. 2 Sketch of a washing machine with notations for functional components. The bodies are indicated with their respective mass, e.g. m_d for the drum

To the group of SFCs belong the strut springs and the top stabilizing springs (see Fig. 2). Functional components which exhibit mainly damping properties are called DFCs, and in the washing machine the strut friction dampers belong to this group. There are also components in the current washing machine design which have both stiffness and damping of significant amount, SDFCs. This group comprises the lower and upper bushings of the washing machine as well as the rubber feet. See Fig. 2 for details.

A graphical topology description of the multibody system modeling a washing machine is depicted in Fig. 3. The symbols used in the topology map are similar to what exists in the MSC.Software/Adams environment; hence users of this software will recognize much of the components directly.

The load of the washing machine is placed into the drum at a fixed location relatively to the drum. The drum, which is a rotating cylindrical body, is connected to the tub via a revolute joint placed at the back end. The revolute joint models the system of two deep groove ball bearings that suspends the drum in the back end of the tub. Also connected to the tub is the motor which drives the rotation. There is a belt drive with a transmission ratio of 1:11, meaning that the motor turns 11 times for one complete turn of the cylinder.

The tub body comprises of the water container, back and front ends (with the hatch). Also the front weights and the motor are included in the tub body. The tub stands on four struts which each comprise in upper and lower bodies. To eliminate a few degrees of freedom and hence the reduce dimension of the model and improve calculation speed, rotation around this axis for the strut cylinder and piston can be constrained. The same goes for all four struts in both upper and lower mounting positions. In this way the rubber bushings describing the connections to piston and cylinder connection to around their own axes with respect to the tub in the case of the piston and with respect of the to the housing in the case of the cylinder does not have to be modeled. Each piston is connected to the tub body via a Hooke joint eliminating rotational motion around the longitudinal axis of the piston. The relative rotational and translation degree of freedoms were eliminated to reduce model size as their impact was deemed to be small.

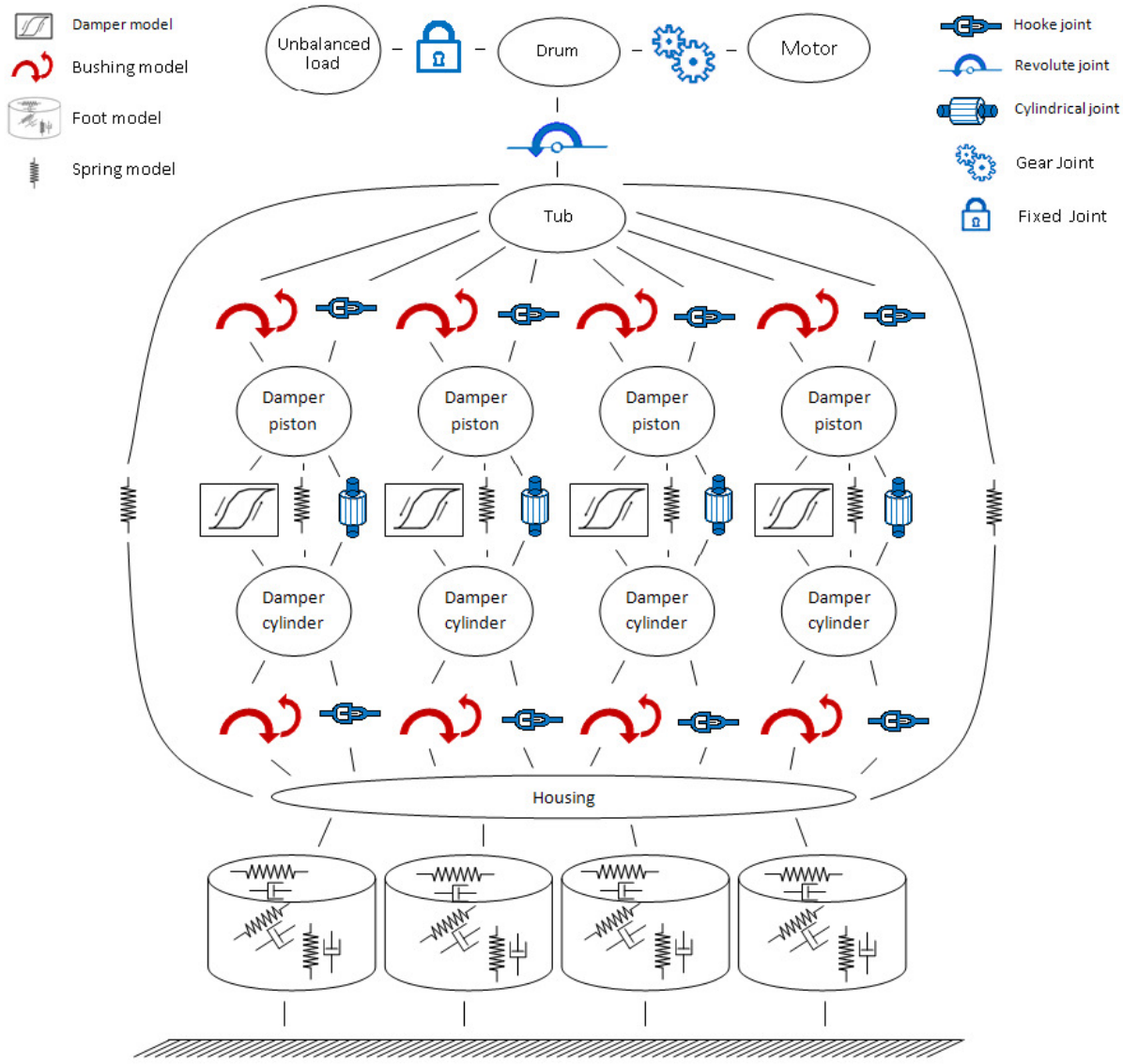

Fig. 3 Topological description of the multibody system of the modeled 4-strut washing machine

The piston and the lower body of the strut, the damper cylinder, are connected with a cylindrical joint. The damper cylinder is in its turn connected to the housing of the washing machine in the same way as the piston is connected to the tub, i.e. with a Hooke joint eliminating the rotation rotational around its longitudinal axis and translation with respect to the housing. The housing part comprises all accessory parts rigidly mounted to the housing, namely: waste water pump, valves, detergent box, electronics, panels etc.

The above written describes the multibody system which is used to model the washing machine depicted in Fig. 1.

3 Computational model

3.1 Mathematical modeling of functional components

Inertial functional components

IFCs are modeled as rigid bodies with parameters: mass, tensor of inertia, position vector for the center of mass, and the Euler angles describing orientation of inertia axes. The following IFCs with respective parameters are included into the washing machine model:

- the drum with $\{m_d, \mathbf{I}_d, \mathbf{x}_d, \boldsymbol{\theta}_d\}$
- the tub with $\{m_t, \mathbf{I}_t, \mathbf{x}_t, \boldsymbol{\theta}_t\}$
- the unbalanced load with $\{m_u, \mathbf{I}_u, \mathbf{x}_u, \boldsymbol{\theta}_u\}$
- the housing with $\{m_h, \mathbf{I}_h, \mathbf{x}_h, \boldsymbol{\theta}_h\}$
- the motor rotor with $\{m_m, \mathbf{I}_m, \mathbf{x}_m, \boldsymbol{\theta}_m\}$
- the strut pistons with $\{m_{pi}, \mathbf{I}_{pi}, \mathbf{x}_{pi}, \boldsymbol{\theta}_{pi}, i=1,2,3,4\}$
- the strut cylinders with $\{\mathrm{m_{ci}}, \mathbf{I}_{\mathrm{ci}}, \mathbf{x}_{ci}, \boldsymbol{\theta}_{ci}, i=1,2,3,4\}$

All together 13 rigid bodies represent the IFCs of the washing machine. Some of the bodies comprise several construction geometries with corresponding inertia properties. For example the tub system contains the front weights and the stator of the motor and other parts with no relative motion to it.

Stiffness functional components

Each of the four suspension struts comprise several functional components namely a spring, a damper and upper and lower rubber bushings. The spring force F_{ssi} is modeled using the relation

$$F_{ssi} = k_{si} \max(0, z_{i0} - z_i), \; i = 1,2,3,4 \tag{2}$$

where k_{si} is the stiffness constant of spring i, z_i is the compressed length of the spring and the unloaded length of the spring is z_{i0}. The *max* function comes from the liftoff property of the

spring mounting, allowing only unidirectional force from the spring. It is however not likely that it will occur during normal operation in a real washing machine given that the imbalance detection algorithm is working properly.

The stabilizing top springs are in reality pre-loaded in such a way that they center the drum in the housing in the *y* direction. Modeling the preload is done with the geometrical data of unloaded length according to equation

$$F_{stj} = k_{tj}(x_{j0} - x_j), \;\; j = 1,2 \tag{3}$$

where k_{tj}, x_j and x_{j0} are the stiffness, current and unloaded length of the spring *j* respectively.

Damping functional components

As mentioned above a strut comprises a friction damper and a spring integrated into one unit. The damping element is a sponge which slides inside a cylinder. The sponge is soaked with grease which makes the sponge slide in a smooth manner. The sponge is swept around a reel shaped cylinder and placed inside the damper cylinder. The amount of damping of a damper is controlled with the diameter of the reel. A large diameter compresses the sponge by and causes a high normal force to the direction of motion. This passive friction damper is a low cost solution, but performs decently. When using friction damping high force is achieved even though the relative velocity between the piston and damper cylinder is low, meanwhile the force is kept relatively low at high relative velocity. For an ideal friction damper the force would be constant, but experience has shown that it is wise to assume that some velocity dependence is present, even though this is undesired from the designer's point of view. Below, several mathematical models of the friction damper are presented. These models were selected, developed and adopted to be used for computer simulation, analysis, optimization and control of vibration dynamics of the washing machines.

The most classic model, and most often a starting point, is to describe the friction as Coulomb dry friction

$$F_i^C = F_{0i}^C \operatorname{sgn}(\dot{z}_i), \;\; i = 1,2,3,4 \tag{4}$$

where F_{0i}^C is the dry friction force and $\dot{z}_i$ is the relative velocity of the piston, or the time derivative of the spring length of equation (2) for strut *i*. As the force response of the damper is believed to depend on the velocity of excitation a viscous component is added, forming equation (5) which can be derived from the Bingham plastic model [20]

$$F_i^{C'} = F_{0i}^{C'} \operatorname{sgn}(\dot{z}_i) + C_i^{C'}\dot{z}, \;\; i = 1,2,3,4 \tag{5}$$

where $C_i^{C'}$ is the coefficient of viscous damping.

To avoid the sharp nonlinear effect of a *sign* function of (4), a nonlinear viscous model have been used. The idea to smooth the sharp transition between velocity directions with an *arctan* function is discussed for example in [21]. The model was used by the authors in [22] in which an additional viscous component with the coefficient C_i^s is introduced in parallel to cope with velocity dependence. The model is defined according to:

$$F_i^s = A_i^s \arctan(B_i^s \dot{z}) + C_i^s \dot{z} \;\; i = 1,2,3,4 \tag{6}$$

The constants A_i^s, B_i^s and C_i^s were determined by using experimental data for the modeled dampers.

Another function which can be used for smoothing the sharp transition when the velocity changes direction is the haversine function [23]. In essence the implementation haversine uses the first half period between of a cosine to model the transition. This function can be generalized in terms of point of saturation α_{sat} centered around origin with

$$y_h^*(\alpha, \alpha_{sat}) = \cos\left(\pi \max\left(\min\left(\frac{\alpha - \alpha_{sat}}{2\alpha_{sat}}, 1\right), -1\right)\right)$$

In the case of velocity transition smoothing the velocity is represented by $\alpha = \alpha(t)$. When the velocity reaches $\alpha = -\alpha_{sat}$ the function y_h^* reaches its minimum and its maximum is reached at $\alpha = \alpha_{sat}$. In this way a damper model which is adapted to the smoothing function can be formed in the following form:

$$F_i^h(z) = F_{0i}^h y_h^*(\dot{z}, \alpha_i^{sat}) + C_i^h \dot{z}, \tag{7}$$

where F_{0i}^h is the dry friction force amplitude and C_i^h is the coefficient of viscous damping of strut *i*.

Sometimes friction has been modeled with a differential equation describing the dynamics of some sort of hysteresis. A well known hysteresis model is the Bouc-Wen model [24]. A mathematical damper model formed by a system of equations comprising a Bouc-Wen hysteresis and a viscous dashpot placed in parallel reads

$$\begin{cases} F_i^{BW} = c_i^{BW} \dot{z} + \alpha_i^{BW} x \\ \dot{x} = A_i^{BW} \dot{z} - \gamma_i |\dot{z}| x |x|^{n_i - 1} - \beta_i \dot{z} |x|^{n_i} \end{cases}, \; i = 1,2,3,4 \tag{8}$$

Here c_i^{BW} is the viscous dashpot constant, α_i^{BW} is the coefficient of the evolutionary variable *x* representing the state of the hysteresis for strut *i*. The parameters $A_i^{BW}, \gamma_i, \beta_i$ and n_i which determine the properties of Bouc-Wen hysteresis are explained more detailed for example in

[24]. In [25], the Bouc-Wen hysteresis is included into a system of moving masses connected with springs and damper to describe the dynamics of the friction elements internal dynamics and to further predict the behavior of the damper.

A linear spring coupled in series with a Coulomb friction damper is called a bilinear element or a Jenkins element. By connecting a number of Jenkins elements a lumped parameter model describing a hysteresis with increased accuracy depending on amounts of elements used. According to for example [21] this modeling approach has gained popularity in friction modeling and called the Iwan model. Two possible arrangements of the Jenkins elements are discussed: in parallel or in series. In our paper the parallel arrangement approach is used. To describe the rate dependent damping better a viscous damper is placed in parallel to the Iwan model with *n* parallel Jenkins elements according to Fig. 4.

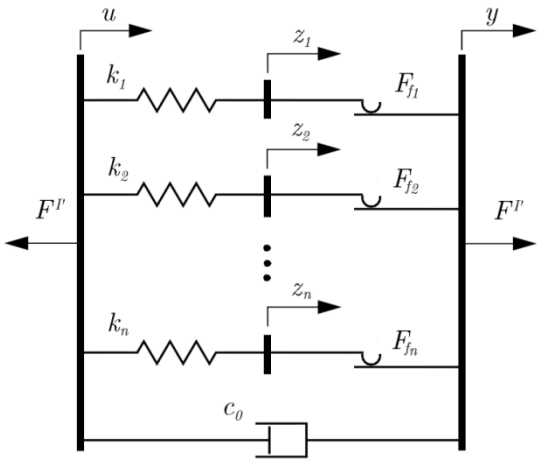

Fig. 4 The Iwan parallel-series based DFC model of degree *n*

Taking the notations from the figure and setting $\dot{y} = y = 0$, the equation describing the force F_k of a Jenkins element with index *k* can be written

$$F_k = k_k \left(z_k - u \right)$$
$$z_k = \begin{cases} z_k^{-} & \text{if } \left| k_k \left(z_k^{-} - u \right) \right| < F_{fk} \\ \dfrac{F_{fk}}{k_k} \operatorname{sgn}\left(\dot{z}_k^{-} \right) + u & \text{else} \end{cases} \tag{9}$$

Here F_{fk} is the dry friction force and z_k is the state variable which unchanged from previous state z_k^{-} if the Coulomb element sticks or updated if sliding occurs in the element. A summation of the forces for the *n* Jenkins elements and adding the viscous damper results in the following equation for the *i*-th foot.

$$F_i^{I'} = \sum_{k=1}^{n} F_{ik} + c_{i0}\dot{u}_i, \; i = 1,2,3,4 \tag{10}$$

where F_{ik} is calculated according to equation (9) for every i-th foot. Each individual Jenkins element will produce a parallelogram shaped hysteresis with height and slopes depending on the parameters F_{fk} and k_k. In Fig. 5 the forces from five individual elements are plotted against displacement to form a hysteresis. The sum of the forces from the elements and the viscous dashpot is plotted to illustrate the shape of the model output. In general it can be said that if the more elements used the smoother the resulting hysteresis becomes.

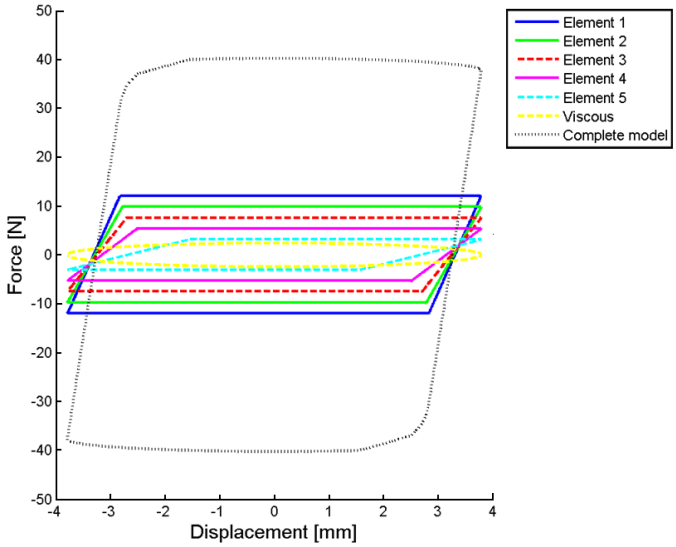

Fig. 5 The forces from dashpot and five individual Jenkins elements together with the Iwan based model

There are also other approaches trying to describe the dynamics of the friction damper focusing on accurate description of stick and slip behavior, such as [26, 27]. This type of formulations is common in the literature and might improve the prediction of the overshoot which can be observed in the measurement data. In the future an extension of some of the proposed models with this feature might be done with little effort. The focus of the damper modeling has however been put on excitation amplitude and frequency impact on the damper force. This aspect is generally not treated with addition of stick slip behavior. The section was focused on friction dampers as the current modeled machine has dampers of this type, but is should be said that even though the friction damper is still the most common type of damper on the market other solutions have been proposed. Such are for example free-stroke dampers from [28, 29] or frequency dependent hydraulic mounts [30], as well as active and semi active solutions for damping in washing machines.

Stiffness-damping functional components

The washing machine feet are made by 80^{o} shore rubber and quite stiff. A way to represent this component is to model it with uncoupled one-dimensional translational spring-damper elements (see Fig. 2). In the lateral directions the force is modeled with the linear relation (11) as the rubber is thick in these directions. Quantative measurements have not been executed to show the exact degree of deformation of the rubber component in the lateral directions, but observations of the machine in operation have indicated that in the deformation is at a maximum somewhere around 5% of its thickness. The linear forces in the x-y plane of foot *i* can be expressed as $\mathbf{F}_{xyi}^{foot}$ according to the equation

$$\mathbf{F}_{xyi}^{foot} = \mathbf{K}_i^{lin}\mathbf{x} + \mathbf{C}_i^{lin}\dot{\mathbf{x}},\ i = 1,2,3,4 \tag{11}$$

Here $\mathbf{K}_i^{lin} = diag(k_{xi}^{foot}, k_{yi}^{foot}, 0)$ and $\mathbf{C}_i^{lin} = diag(c_{xi}^{foot}, c_{yi}^{foot}, 0)$ are spring and damper constant matrixes for the foot *i*. Rubber components force response are often nonlinear, if large deformations are present. The construction of the rubber feet of the washing machine is such that the material between the convex head fastening pin and bottom surface is very thin. The thickness of the foot rubber subjected to loading from the pin is 1 mm at its thinnest location in the vertical direction. In addition to this the shape of the bottom surface of the rubber is ribbed. Because of this it is legitimate to assume that a nonlinear characteristic can be influential if the foot is subjected to loading with wide range in amplitude. The vertical force at foot *i* can be expressed as

$$F_{zi}^{foot} = F(z, \dot{z}),\ i = 1,2,3,4$$

This nonlinear foot force is comprised of a nonlinear stiffness component and a damping element. To make the stiffness and damping depend on the excitation the visco-elastic Maxwell model is used. In this context the Maxwell model consists of a single dashpot connected in series with a spring. To enhance the foot model, a dashpot is placed in parallel with the Maxwell model and the nonlinear spring as shown in Fig. 6.

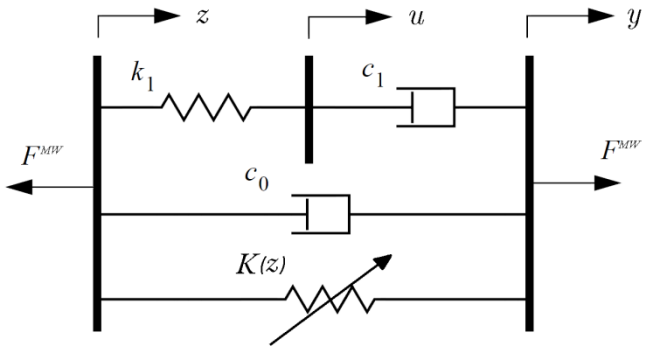

Fig. 6 The nonlinear Maxwell based foot model

To describe the nonlinear stiffness $K(z)$ a cubic polynomial is used. The stiffness is described according to

$$K_i^{foot}(z_i) = p_{i3}z_i^3 + p_{i2}z_i^2 + p_{i1}z_i + p_{i0},\ z_i \in [z_i^{\min}, z_i^{\max}],\ i = 1,2,3,4$$

Here z is the vertical compression of the foot.

The equation of the Maxwell model is written

$$F^{MW'} = c_1(\dot{y} - \dot{u}) = k_1(u - z) \tag{12}$$

Where if $\dot{y} = y = 0$ the force $F^{MW'}$ can be written as

$$F^{MW'} = -c_1\dot{u};\ \dot{u} = \frac{k_1}{c_1}(z - u) \tag{13}$$

which together with an elastic part with stiffness from (14) and the damping from a dashpot with coefficient c_0 forms the suggested foot model for vertical compression of a foot according depicted in Fig. 6 as

$$\begin{cases} F^{MW} = zK(z) + c_0\dot{z} + c_1\dot{u} \\ \dot{u} = \dfrac{k_1}{c_1}(z - u) \end{cases} \tag{14}$$

Combining the equations **Error! Reference source not found.** and (14) the total force for all three directions can be written as

$$\mathbf{F}_i^{foot} = \mathbf{K}_i^{lin}\mathbf{x} + \mathbf{C}_i^{lin}\dot{\mathbf{x}} + F^{MW}(z,\dot{z})\mathbf{e}_z,\ i = 1,2,3,4$$

Here $\mathbf{e}_z$ is a unit vector of the vertical direction.

The rubber bushings which connect the strut to the tub mounting are modeled as a rotational springs together with damping proportional to the rotational angle deflection velocity of the bushing. The local coordinate system which indicates the orientation of the strut cylinder at equilibrium position of the rubber is called x'y'z' (fixed to the housing) and oriented so that

the y' axis is parallel to the y axis of the housing and the *z*' axis is oriented in line with the strut (see Fig. 2). In this way the rubber components does not have to include torque around the *z*'-axis. No torque around this axis gets transferred from the piston to the cylinder as the piston is free to rotate inside the cylinder. Using the notations from Fig. 2 the torque at the lower rubber bushings is described with the equation

$$\mathbf{T}_i^l = \mathbf{K}_i^l \boldsymbol{\theta} + \mathbf{C}_i^l \dot{\boldsymbol{\theta}}, \; i = 1,2,3,4 \tag{15}$$

Here $\mathbf{K}^l = diag(K^l_{x'i}, K^l_{y'i}, 0)$ and $\mathbf{C}^l = diag(C^l_{x'i}, C^l_{y'i}, 0)$ are the stiffness and damping matrices for the lower bushing torque of strut *i*. The bending angles $\boldsymbol{\theta}$ are taken from the deflection of the strut with respect to the local coordinate system *x'y'*z' of the housing. The vector $\boldsymbol{\theta}$ is the result of the projection of the bending of the strut onto the two axes and from this the reaction force is calculated. A linear approach was used with the purpose of easy scalability for later model usage in optimization and to reduce model complexity. In the same way as described above the equation for the upper rubber bushings with properties according to $\mathbf{K}^u = diag(K^u_{x'i}, K^u_{y'i}, 0)$ and $\mathbf{C}^u = diag(C^u_{x'i}, C^u_{y'i}, 0)$ are formulated.

3.2 Computer implementation

By using the developed FCs mathematical models the computational model of a washing machine is implemented in the commercial software Adams/View from MSC.Software. One reason for the selection of this computational environment is the visual feedback of the kinematics and dynamics of the model the software provides. By using this capability model debugging is greatly facilitated. The other reason is compatibility with drawings produced in CAD-Software. The IFCs of the washing machine model are determined based on CAD drawings which are taken from production and research machines. Mass and inertia can in this way be automatically calculated given a density of the material a part is created of. This gives the model a flexible and at the same time robust definition of mass and inertia properties. By robust, it is meant that there is a visual update of the model if a part with different geometry is used in the model. Also specification and checking of locations of joints or other constraints is facilitated as their exact location and orientation are indicated in the model with icons. The computational model is built in a modularized way meaning for example that multiple definitions of several parts can be used. Examples of this are different counterweight designs which have a big impact on inertia properties of the system, or different detergent boxes which have impact on collision detection values but do not affect the computational model in any significant way.

Building a model in the Adams\View environment is started by importation of drawings and creation of model bodies, called parts in Adams. A part can consist of different drawings in Adams as long as all the geometries have the same density. If two drawings with different densities are to describe the geometry and inertia of one thought part then one must (normally) give up the inertias parametric dependency on the geometry and assign properties manually, If one wants to keep the parameterization then a fixed joint could be applied between two model bodies and hence increase the complexity of the system (with 6 additional generalized coordinates – 6 constraints = 0 degrees of freedom). Naturally this solution will demand extra computational power and should be avoided if not the connection forces between the parts are of interest and the parameterization capability can be discarded. There are workarounds which keeps the flexibility and at the same time does not introduce constraints or generalized coordinates but these will not be described here.

The Adams implementation of the physical machine which is shown in Fig. 1 is depicted in Fig. 7. In the figure also a detailed view of one of the strut and its connection to the other parts is given.

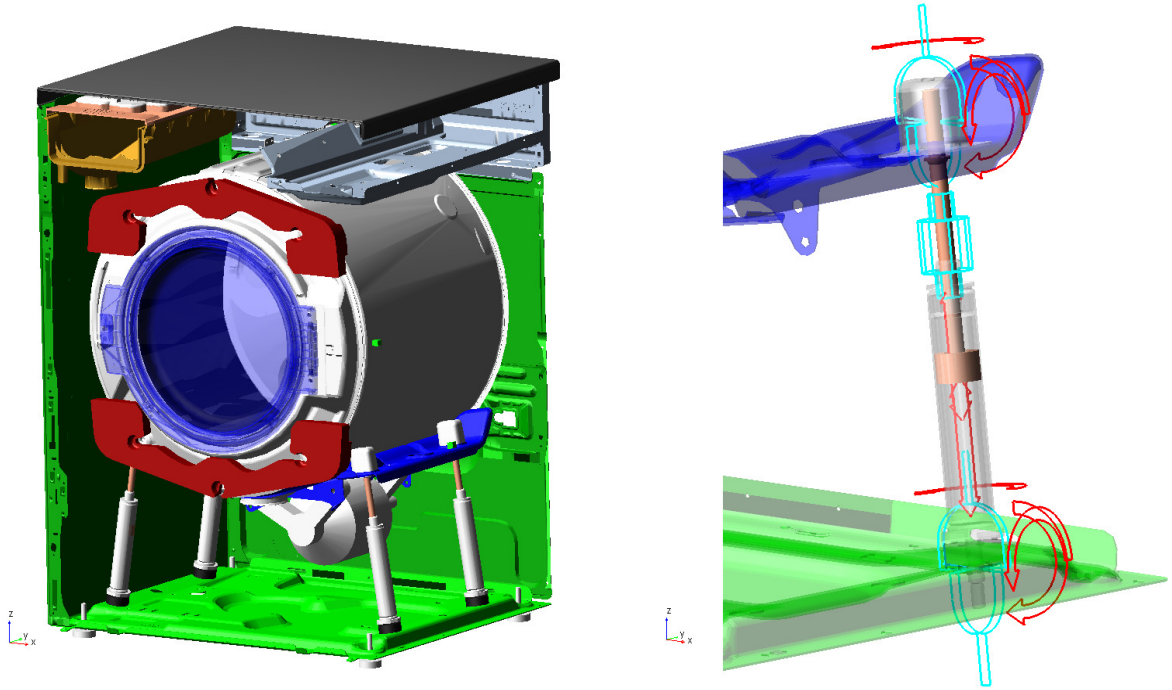

Fig. 7 The computational MBS model and a detailed view of a strut showing icons representing constraints, force and torque vectors

Some of the icons in the figure can be recognized from the topological description given in Fig. 3. One exception is the damper model which in Adams is depicted by a bidirectional arrow (SFORCE). Also the spring model is in the same environment depicted in this way.

In Adams, to define how the model is constructed and how different components should be interconnected, each functional component and constraint has one or more coordinate systems coupled to it. For IFC:s only one coordinate system is enough to define location and orientation of mass and inertia properties respectively. For constraints one coordinate system is fixed on each affected part. The coordinate systems are in Adams called “markers”. By using functions using these markers as arguments various constraints can be created. Consider for example a cylindrical joint applied between two parts which are connected at a point P. At this point two markers M1 and M2 respectively belonging to each of the part are defined with an orientation fitting the desired orientation of the joint. The cylindrical joint equivalent constraint is then defined by three equations DX(M1,M2)=0, DY(M1,M2)=0, AZ(M1,M2)=0, where DX and DY are functions which measure the distance between two markers in respective direction, and AZ is a function measuring the enclosed angle between the $\mathbf{e}_z$ vectors of the two coordinate systems. When it comes to force functional components the function is similar. The distance (translational or angular) “between” two markers and is can be used when defining a spring and are used to define where the action and reaction forces should be applied.

The modular construction of the washing machine computational model comprising a set of functional components is illustrated in Fig. 8. In total two complete production machines and two physical prototype machines have been implemented in the environment. By setting switches and running macros, different parts or sets of parts and/or structural components can be used. Multiple versions of components used in different machine models are defined and placed in the database. In this way they are made available for selection and incorporation in the model with a switch variable. Structural components like dampers and springs are defined in the same way. Also whole units like struts can be turned on and off and in some cases also moved, as of the moment a total of 8 struts can be used at the same time in the model.

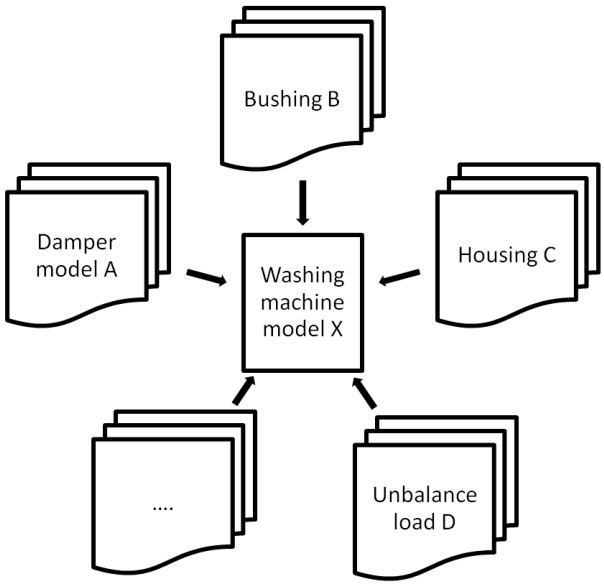

Fig. 8 The modular construction of the washing machine computational model comprising a set of functional components

This flexibility together with the multiple mathematical models of each damper enables that a lot of different suspensions systems can be represented in the washing machine computational model. In the database, groups of switches have been defined corresponding to different in production or prototype machines. In this way the environment quickly can be set up to model a given washing machine. The idea of easy parameterization to facilitate analysis and optimization has similarities with for example [31].

Analysis of the description of a washing machine mechanical model, system functional components and imposed constraints leads to a conclusion that the washing machine is modeled as a controlled mechanical system comprising 13 rigid bodies with constraints removing 66 degrees of freedom, giving the system totally 12 degrees of freedom. In state space representation the dynamics of considered washing machine is described by the system of differential equations

$$\dot{\mathbf{x}} = \mathbf{f}(\mathbf{x}, t, \mathbf{p}, \mathbf{d}, \mathbf{u}) \tag{16}$$

with initial conditions

$$\mathbf{x}(0) = \mathbf{x}_0 \tag{17}$$

Here $\mathbf{x} = [x_1, x_2, x_3, ..., x_{24}]^T$ is the 24-dimensional vector of state variables, $\mathbf{p} = [p_1, p_2, p_3, ..., p_{N_p}]^T$ is the N_p-dimensional vector of given system structural parameters, $\mathbf{d} = [d_1, d_2, d_3, ..., d_{N_d}]^T$ the N_d-dimensional vector of washing machine design parameters, and $\mathbf{u} = [u_1, u_2, u_3, ..., u_{N_u}]^T$ is the N_u-dimensional vector of external control stimuli, e.g. forces and

torques acting on the system, spinning speed, etc. The output of the computational model is a vector of dimension N_y defined by $\mathbf{y}=\mathbf{g}(\mathbf{x},t,\mathbf{p},\mathbf{d},\mathbf{u})$. The vector function **f** is specified internally inside Adams environment through the implementation of the computational model. Here also the vector function **g** also is specified according to standard Adams results set and with additional user specific measure functions. The initial state $\mathbf{x}_0$ is given in terms of initial positions and initial velocities. The corresponding equilibrium positions are not necessarily the same as the one described by positions in $\mathbf{x}_0$. However it is desired for most simulations they are and therefore the preloads of the force components have been designed to give as close as possible equilibrium positions to $\mathbf{x}_0$ as possible. For most usages of the washing machine model implemented in Adams the calculation is supposed to start at static equilibrium.

Different parameters can be considered as components of vectors **d** and **p**. For instance, the components of vector **d** can be stiffness of springs in struts, rubber bushing stiffness and damping, damper position, etc. Inertia of the drum, housing and other parameters which should be considered given at all times comprise the vector **p**.

Adams/View handles the solving of the initial value problem (16) and (17), i.e. calculation of state variables and output vector. The results can be animated to visually inspect the motion of bodies and motion signature characteristics of a particular suspension system.

In the software a collision detection capability is built-in, giving the possibility of detecting if a body is colliding with another. This feature works even with the occasionally complex geometry of the CAD drawn bodies. As stated earlier one of the directions of washing machine development and research today is the increase of capacity, which in the standardized outer size white-goods industry means a decrease of empty space inside the housing. Working with this problem one realizes that collision detection is a really useful feature for detection of critical points inside the housing.

4 Experiments, parameter identification and model validation

The methodology used for construction of the washing machine model relies on models for functional components used in the suspension system and its structural parts. Important parts of the selected methodology for modeling are the experiments on components. Experiments on each isolated component have been done in test rigs giving understanding about their respective dynamic properties.

4.1 Description of test rigs

Component measurements

A test rig designed for dynamic measurements on the force response of objects exposed to small displacement excitation is available at the department. The test rig which is displayed in Fig. 9 can periodically compress the test subject kinematically with an excitation speed from 5 up to 200 Hz with amplitude of up to 0.5 mm. Hence it is suitable to be used for measurement on the feet of the washing machine. The foot compression is measured with laser displacement sensors with a resolution of 1µm together with the force with a sampling frequency of 10 kHz. The excitation is kinematic meaning that the resulting force depends on the rubber properties. For harder test subjects the rig can excite with forces up to several thousand Newton. The data is sampled with a CompactDAQ NI-9172 system and processed with software built in Labview from National Instruments Inc.

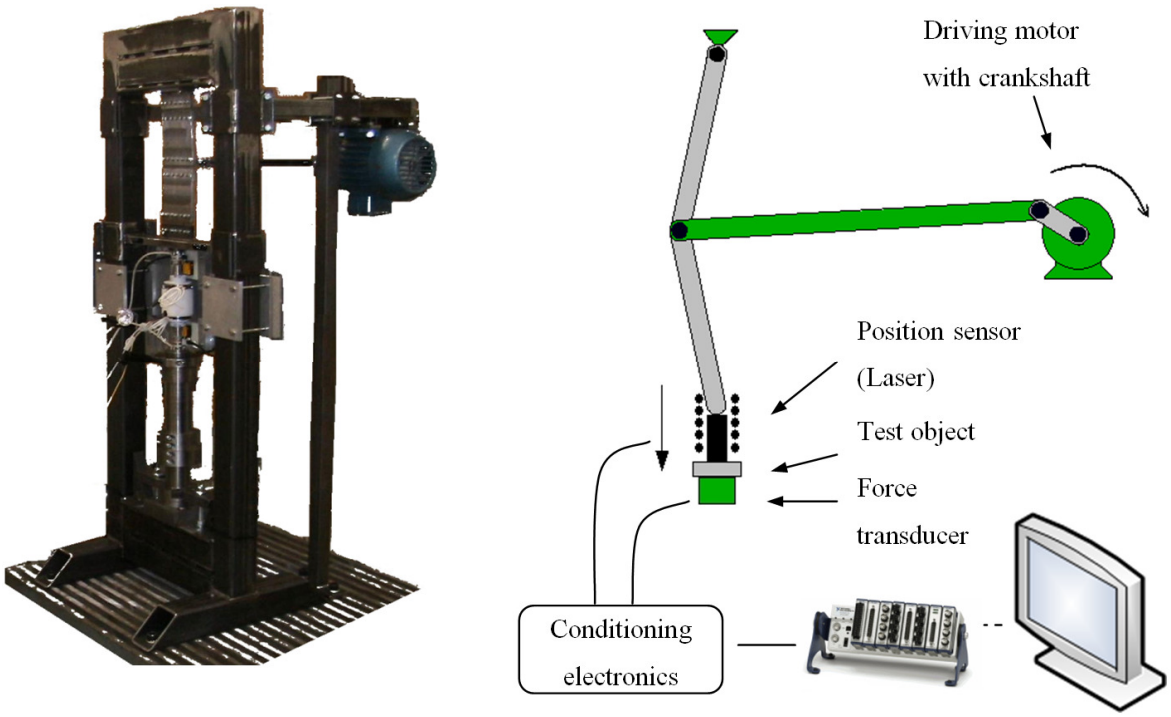

Fig. 9 Equipment used for foot experiments: a) The test rigs and b) a sketch of its measurement system

The test rig has been used for measurement on the rubber foot in vertical direction. During the experiments data was sampled at steady state excitation with amplitudes and frequencies corresponding to different operational conditions of the washing machine around a preload force corresponding to the weight of the machine.

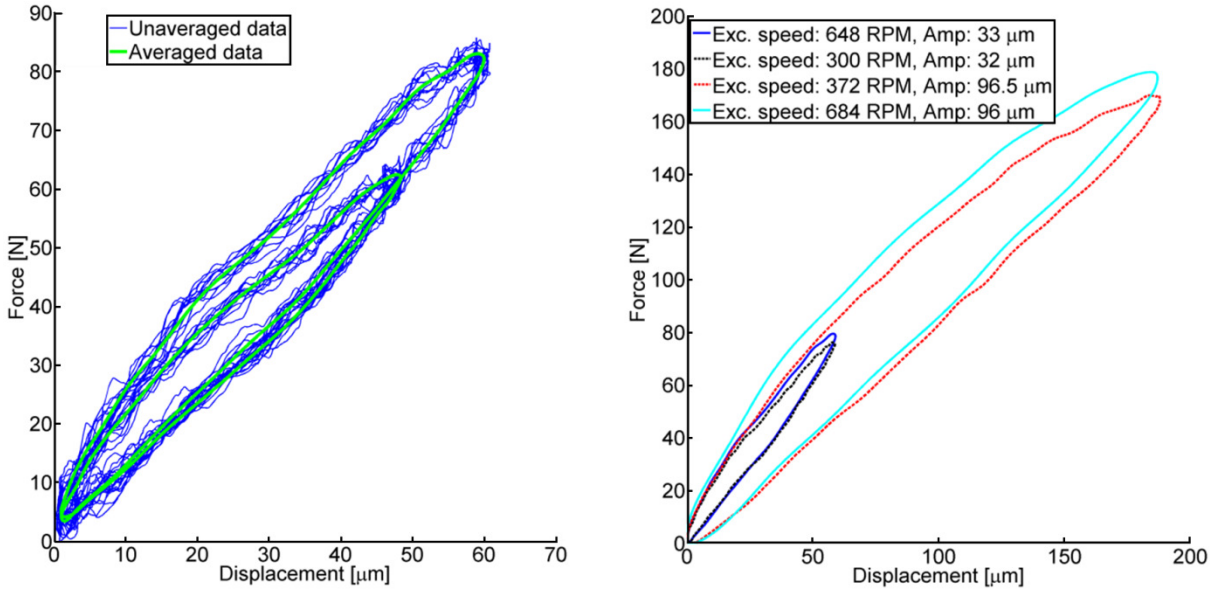

Fig. 10 Data acquired with the test rig for washing machine feet: a) Unaveraged and averaged measurement data and b) averaged data at different excitations

Several experiments were performed on the washing machine feet letting excitation frequency and amplitude vary. The amplitude here is defined as half the stroke length during the experiment. As the force and position signals were rather noisy, and therefore not suitable to use as input for model parameter identification directly. To enable the usage of the data in the modeling procedure a filtering technology was applied. The filtering process consists of acquisition of several periods at steady state conditions at first. Later the force and position are averaged over the periods to give improved smoothness and accuracy. The measurement data before averaging and resulting averaged data are visible in Fig. 10a. In Fig. 10b some of the measurement datasets are plotted showing response at different excitations.

A rig made for classification of damper properties has been developed in cooperation between Asko Appliances AB and Chalmers University of Technology. It is based on a standard test rig used for classification of production struts used for modeling of dampers in [22], but made more rigid and adapted with a frequency converter to cover an excitation range of 0-30 Hz. Regarding amplitude it is possible to test 0 to 25mm. Force and displacement are measured with a load cell and a linear variable differential transformer (LVDT), respectively. Data acquisition is made with a computer running Labview 8.5 equipped with a NI PCI-MIO-16E-4 card. For measurements on the damping functional component the data was sampled during steady state excitation with stroke amplitudes and frequencies corresponding to normal operational conditions. For improved smoothness and accuracy several periods of excitation

were acquired and averaged. The test rig used for experimental study of DFCs is shown in Fig. 11 and described further in [32]

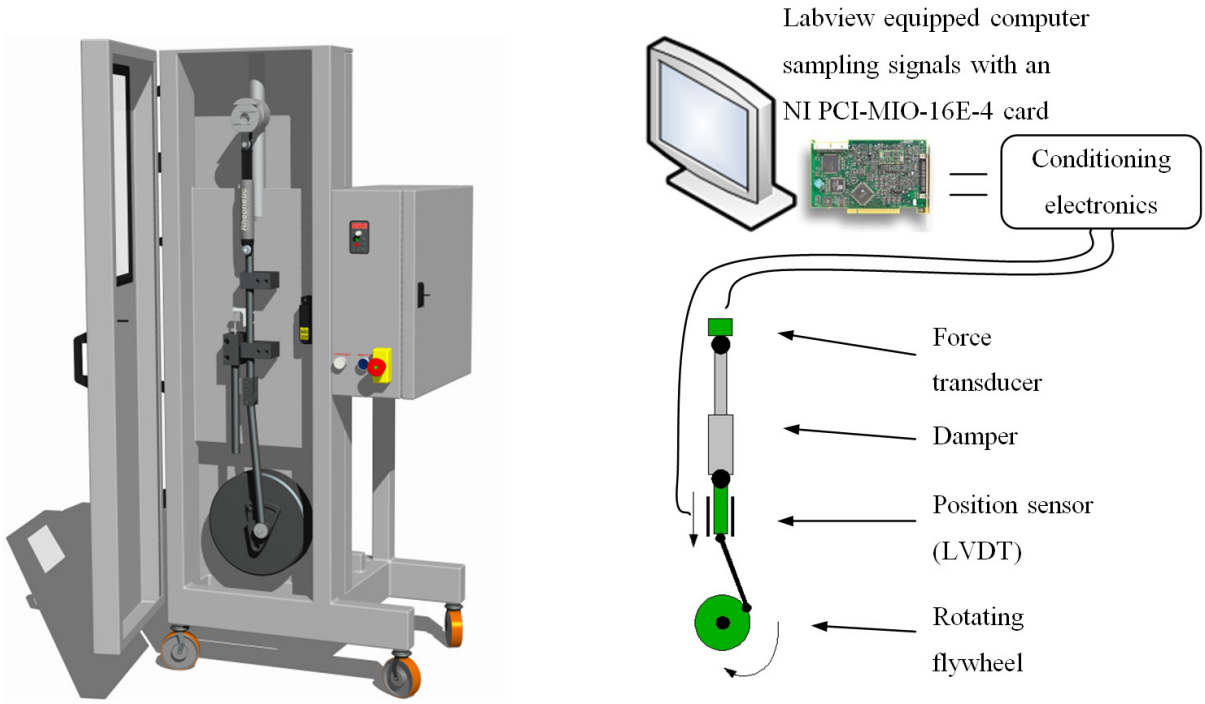

Fig. 11 Equipment used for strut experiments: a) The test rig used and b) a sketch of its measurement system

In Fig. 12 measurement data acquired from experiment done with varying amplitudes and frequency of excitation is displayed. The force dependency on the frequency a) and amplitude b) of excitation can clearly be seen. The inclination of the curves comes from the stiffness of the built-in spring of the strut. Due to the construction of the current strut type it was not possible to test only the damper element inside. Hence during parameter identification building the spring (2) corresponding to the spring in the strut was added to the model.

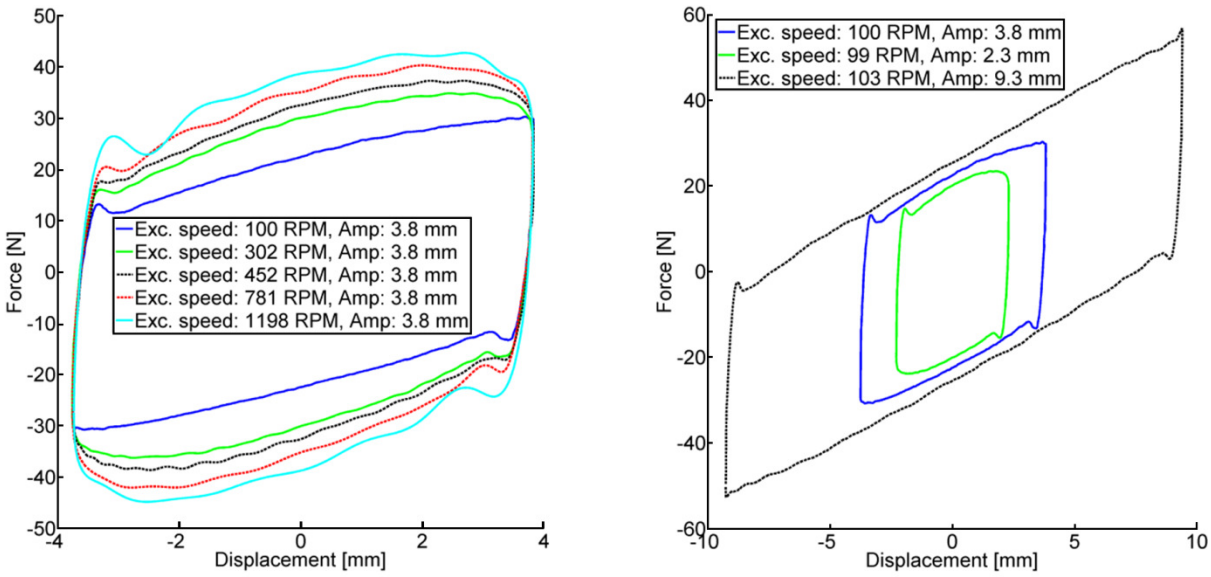

Fig. 12 Data acquired with the test rig for washing machine struts with varying a) excitation speed b) stroke length

The rubber bushings have been tested statically with experiments giving angular deflection-force relations hence static angular stiffness values [33].

Complete machine measurement

During experiments on washing machine vibration dynamics, excitation is given to the system by spinning of the drum which to which an (unbalanced) load has been added. Depending on which type of experiment is to be performed either a number of standardized cotton cloth pieces weighing 100g each, or a number of fixed weights are added to the drum. The first type of load can move freely inside the drum, leading to that the results become unrepeatable, and also to that the distribution of if it at any given time become undeterminable. It is suitable and has been used for water extraction performance experiments [34], load distribution experiment [35], but it is not suitable for model building experiments. The fixed weights imbalance is created by adding steel plates with predetermined weight to a holder or by sticking lead weights to the drum using double adhesive tape.

In the test rig the machine stands on four load cells fastened to a heavy block which provides adjustability of the foot positions when testing machines with different foot locations. The test rig and measurement system is depicted in Fig. 13. In Table 1 the different measurement signals that can be collected and the signals that can be used to control the washing machine is listed.

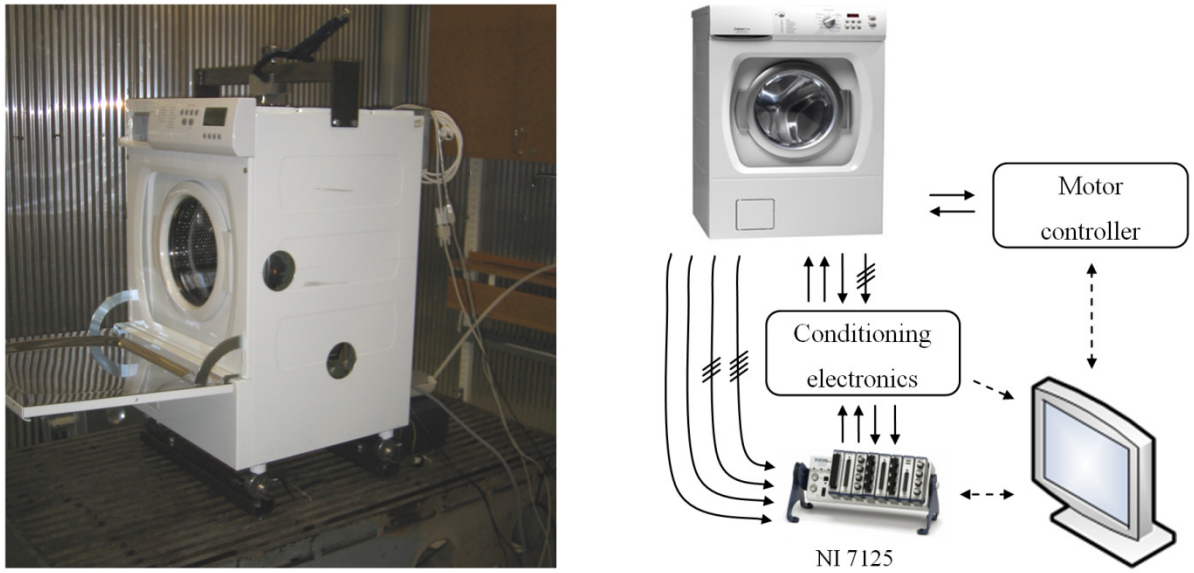

Fig. 13 The complete machine test rig used for experiments on the washing machine a) used to measure on an Asko Cylinda FT 58 and b) sketch of the measurement system

Under each foot a force sensor is placed making it possible to measure the forces individually under static and dynamic conditions. The accelerometers are used to measure the drum's vertical and lateral accelerations and the acceleration of the tub-strut connection part. A touch less hall-effect sensor is used to measure the displacement in three translational directions. Additional sensor control semi active damper if the machine tested is equipped with such an actuator. The washing machine waste water pump can be controlled from the computer during experiments with water such those done in [34]. A load cell based scale can be used to measure the extracted water amount during spinning for analysis and optimization of the spinning sequence.

To acquire and condition input signals and output control National Instruments software LabView were used together with of the shelf hardware and custom built hardware for the specific measurements.

Table 1 Measurement equipment connected to the rig indicating type and whether it provides an output or demands a control signal

Type	Model	Serial no.	Position	I/O	Measuring/controlling
Load cell	CTS63100KC35	312281	Left front foot	O	Vertical force, F_z^{LF}
Load cell	CTS63100KC35	0205	Left back foot	O	Vertical force, F_z^{LB}
Load cell	CTS63100KC35	313303	Right front foot	O	Vertical force, F_z^{RF}
Load cell	CTS63100KC35	200063	Right back foot	O	Vertical force, F_z^{RB}
Accelerometer	B&K4507	10881	Top back of tub	O	Vertical acceleration, $\mathbf{a}_{1z}$
Accelerometer	B&K4507	2054257	Front right of tub	O	Lateral acceleration, $\mathbf{a}_{2y}$
Accelerometer	B&K4508	1937280	Support part	O	Acceleration, $\mathbf{a}_3$
Induct. sensor	M12KS04-WP-C1	-	Drive pulley	O	Tachometer signal, N
Hall sensor	N/A	-	Top center of tub	O	X-Y-Z displacement, $\mathbf{X}^{P_{TC}}$
PWM controller	Lord Wonderbox		-	I	Damper voltage, u_d
Current sensor	-	-	-	O	Damper current, i_d
Pump	-	-	-	I	Wastewater pump
Load Cell	N/A	-	-	O	Extracted Water, m_W
Motor controller	AKO	-	-	I/O	Motor speed, ω
					Estimated imbalance, m_u^{est}
Data acquisition	NI7125	HA4319698	-	I/O	Sample frequency, f_s

The signal quality of the resulting spin-speed originating from the mounted tachometer is high giving up to 24 pulses per revolution from which the speed of the drum can be calculated with good resolution. With help of this signal forces and displacements can be plotted as functions of rotation speed instead of as functions of time. In Fig. 14 is the motion of the point P_{TC} in the *x*-*z* plane plotted. The motion has been divided into time segments to show more clearly the formation of thee oval shaped trajectory of the point motion. Generally it can be said that the inclination is dependent on the direction of spinning, which in this example was anti-clockwise when observing the drum from its front. The data has been truncated at t=20 seconds to show the more interesting part of motion when concerning the tub. At t>20 the motion remain at a steady state forming a similar ellipse to what can be seen in the plot of the last time section. In Fig. 15 the vertical force measured at the four feet is displayed. In the figure the force has been plotted with the rotational speed of the drum on the x-axis to show at which frequencies the foot forces reach critical levels. Desired constant spinning speeds to perform longer time water dehydration can be chosen for example based on the levels of

forces available in the figure the feet. Noted should be that the powerful resonance at a spinning speed of 800 rpm has little effect on the motion of the tub. Experiments have shown that the forces come from motion of the housing, possibly due to flexion of the housing structure.

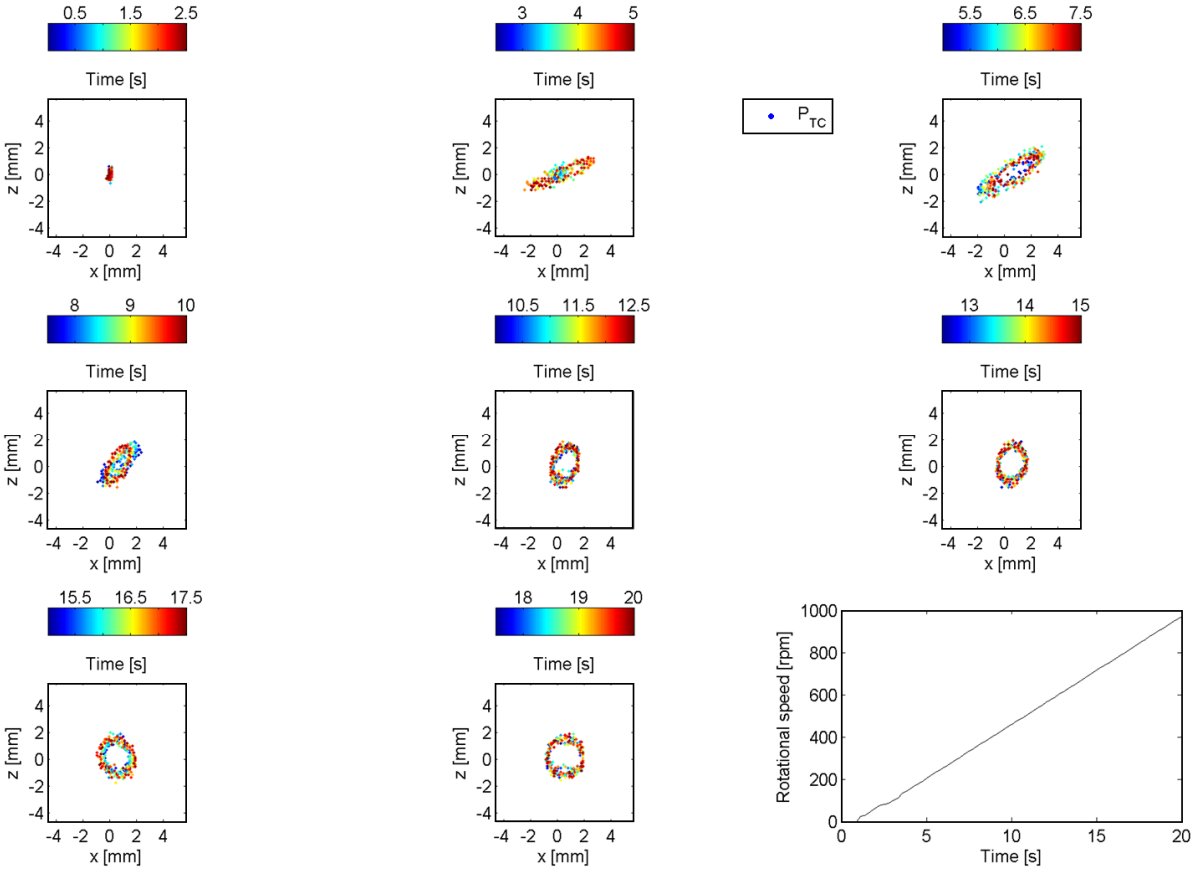

Fig. 14 Motion of point P_{TC} in the x-z plane divided into time segments for a ramp in rotational speed

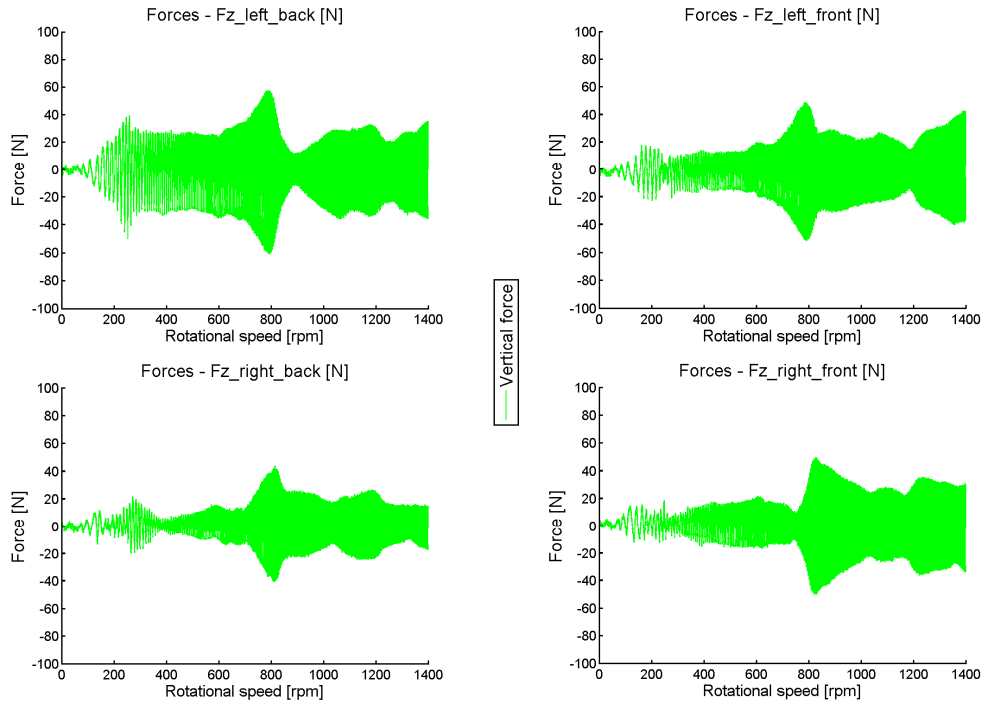

Fig. 15 Forces at the four feet as plotted with rotational speed on x-axis

The data in both Fig. 15 and Fig. 16 belong to the same measurement and the vibrations are exerted by an imbalance according to Table 4.

4.2 Functional components parameter identification

In the previous chapter the functional components of the washing machine have been introduced and their internal dynamics described by respective mathematical models. Each model comes with a set of parameters which has to be tuned to the physical components of the modeled machine. That is, to be able to implement the mathematical model (16) and (17) into the computational model of the washing machine, the model parameter identification problem has to be solved. To solve this problem several test rigs were built (described above) and experimental data of performance of the functional components of the washing machine have been gathered and analyzed.

The functional component model parameter identification problem is stated as an optimization problem where an error function is minimized. The optimization toolbox of Matlab was used to solve the corresponding optimization problem. Concerning statements of parameter identification problems and formulations of error functions, there exist many different approaches depending on applications, see e.g. [37-39]. Inspired by [37-39] the normalized root mean square deviation error for an experiment j is used and written as

$$E_j = \frac{\sqrt{\frac{1}{N_j}\sum_{i=1}^{N_j}\left(F_j^{Model}(i) - F_j^{Exp}(i)\right)^2}}{\sqrt{\frac{1}{N_j}\sum_{i=1}^{N_j}\left(F_j^{Exp}(i) - \overline{F_j^{Exp}}\right)^2}} \tag{18}$$

where F_j^{Model} is the modeled force and F_j^{Exp} is the measured force, where N_j is the number of data points in measurement *j*, $\overline{F_j^{Exp}}$ is the average the measured force at measurement j. As several experiments at different conditions have been performed an estimation of how the model performs at all conditions is interesting.

Averaging the error over all experiments can be done according to

$$E_M = \frac{1}{M}\sum_{j=1}^{M} E_j \tag{19}$$

where *M* is the number of experiments performed.

The main purpose of a damper in a mechanical system is to dissipate energy. Hence, it is important that the amount of energy that the model dissipates agrees with the amount of energy dissipated during measurement. For one cycle the energy dissipated is corresponding of to the area enclosed by the force-displacement plot. A relation for the estimation of relative error for the average error energy dissipation has been formulated as follows

$$E_E = \frac{1}{M}\sum_{j=1}^{M} \frac{\left|\int_{z_1}^{z_2} F_j^{Model} dz - \int_{z_1}^{z_2} F_j^{Exp} dz\right|}{\int_{z_1}^{z_2} F_j^{Exp} dz} \tag{20}$$

Here, z is the displacement and z_1 and z_2 are the displacement bounds. Using the obtained experimental data, the parameters of the damper models described in previous chapter were determined by the optimization toolbox in Matlab. The models together with datasets for a damper, comprising 10 different excitations by displacement and frequencies, were passed though the optimization algorithm determining the constants which minimized the model error according to (19). In Fig. 16 and Fig. 17 measurement data for two different excitation cases are presented together with the fitted models defined by equations (4), (7) and (10) respectively. As can be seen in Fig. 17, it is clear that the pure Coulomb friction model (4) greatly underestimates the force at the higher rotation frequency. To estimate quantitatively the obtained solutions of the model identification problems normalized relative errors E_M, for the different models of the strut damper as well as normalized energy dissipation errors, E_E, are presented in table 2. Closest response to the measurement data is obtained by using the Iwan-based model (10), then the Bouc-Wen model (8) followed by the *haversine* smoothed

model (7) which performs similarly as the *arctan* smoothed model (6). Regarding energy dissipation the Iwan-based model also performs best but is here followed by the smoothing function based models (6) and (7).

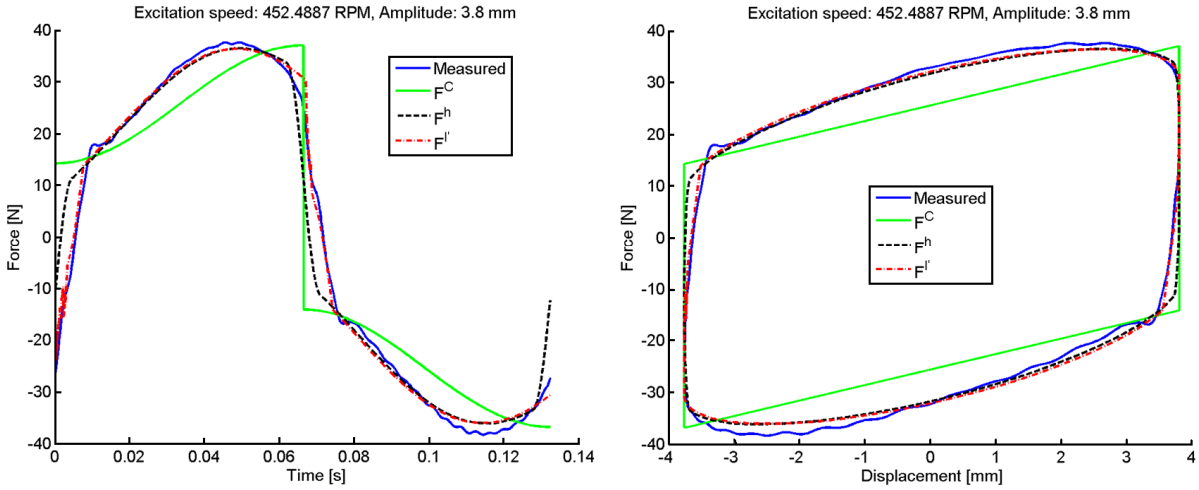

Fig. 16 Measurement data of one of the damper and output data from the models at 452 rpm excitation speed

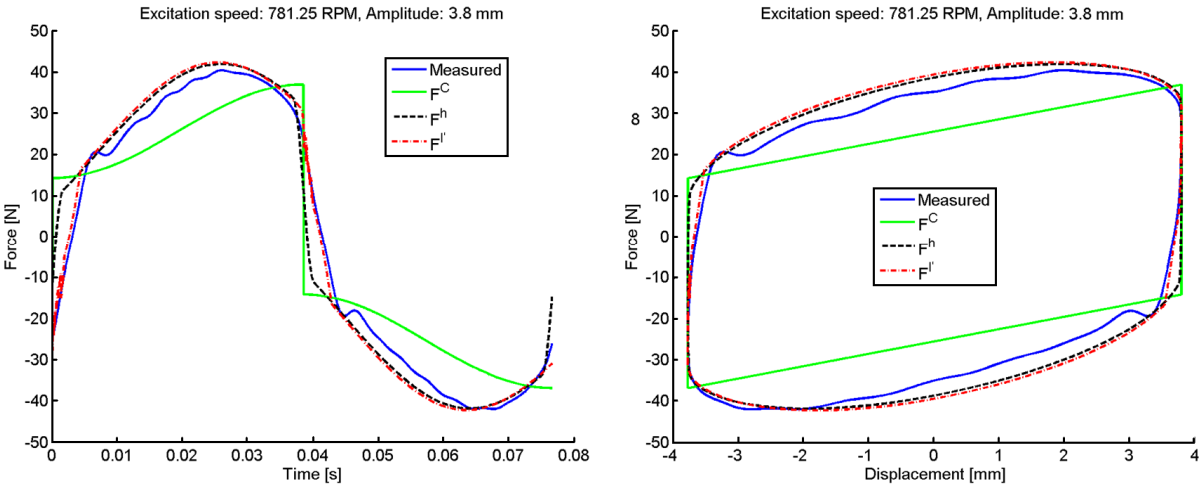

Fig. 17 Measurement data of one of the damper and output data from the models 781 rpm excitation speed

Table 2 Relative errors for the different models describing the strut damper

Error measure	F^C	$F^{C'}$	F^s	F^h	F^{BW}	$F^{l'}$
Force prediction, E_M (%)	35.8	23.8	18.8	19.4	16.8	8.5
Energy dissipation, E_E (%)	15.3	10.8	5.3	5.2	6.8	5.0

The parameters of the respective models found when minimizing the cost function (18), for one of the tested dampers, was for the Coulomb dry friction damper model (4): $F_0^C = 25.6$ N, for the Bingham based model (5): $F_0^{C'} = 15.1$ N, $C^{C'} = 0.100$ Ns/mm, for the smoothed sign model (6): $A^s = 16.5$ Ns/mm, $B^s = 0.0671$, $C_i^s = 0.0429$ Nmm/s . For the haversine model (7):

F_0^h = 20.0 N, α^{sat} = 36.5 mm/s, C^h = 0.0677 Ns/mm, for the Bouc-Wen model (8): c^{BW}=0.0791 Ns/mm, α^{BW}=10.6 Ns/mm, A^{BW}=10.6, γ=–1.90 mm^{-2}, β=7.63 mm^{-2} and n=1, and for the Iwan based model (10): F_{f1}=3.25 N, k_1=16000 N/mm, F_{f2}= 5.30 N, k_2=429.0 N/mm, F_{f3}=4.00 N, k_3=50.6 N/mm, F_{f4}=4.37 N, k_4=29.1 N/mm, F_{f5}= 2.59 N, k_5= 16.6 N/mm C_0=0.0738 Ns/mm.

Similarly the parameters of the foot model were estimated from measurement data using the Optimization toolbox of Matlab to minimize the model error compared to dynamic measurements according to (19). In Fig. 18 two sets of measurement data for foot dynamics are displayed together with data from the different models.

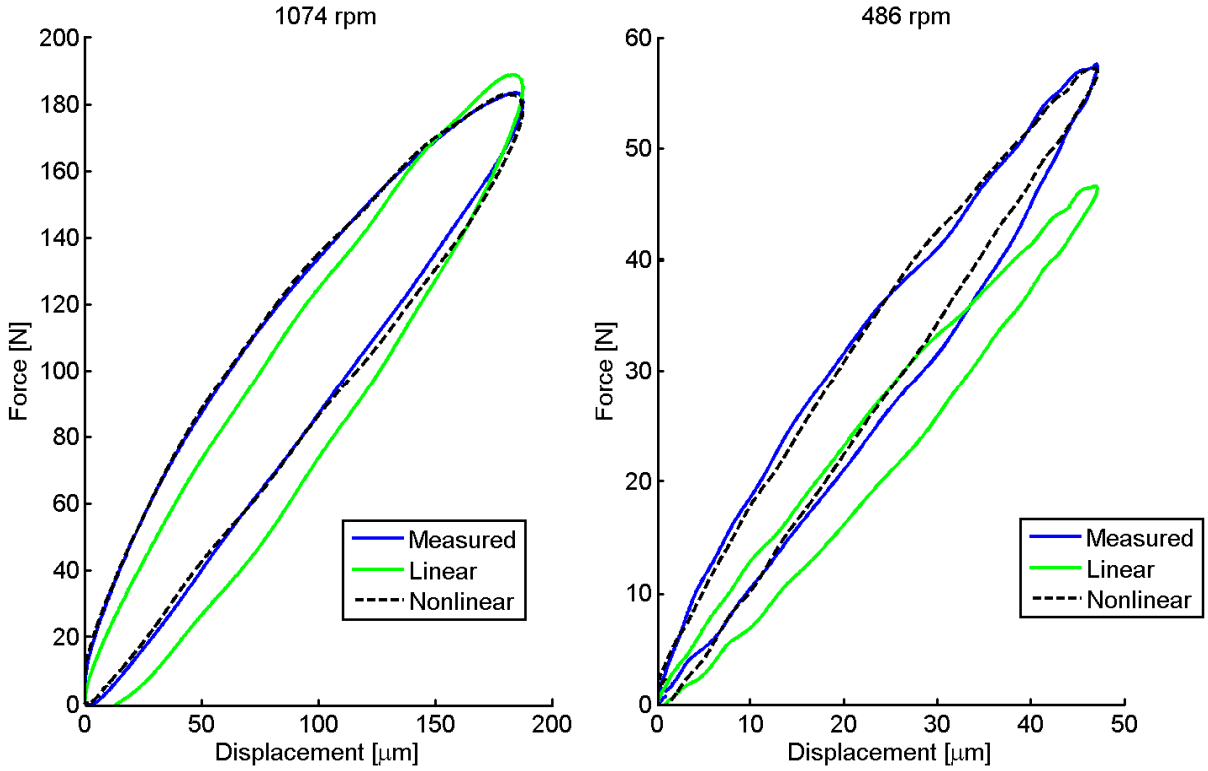

Fig. 18 Measurement and data of models for foot dynamics

In the figure the linear model´s failure to describe the stiffness is clearly visible, whilst the nonlinear Maxwell model predicts the force fairly well for the different excitations.

Table 3 Relative errors of prediction for foot models

Error measure	F^{lin}	F^{MW}
Force prediction, E_M (%)	14.6	5.6
Energy dissipation, E_E (%)	29	13

The identified values of the parameters of the Maxwell based model described by equation (14) which minimize the cost function (18) are k_{0i}= 172 N/mm, c_{0i}= 32.6 Ns/mm, p_{1i}= -1870

N/mm, p_{2i}= 13800 N/mm, p_{3i}= -413 N/mm, p_{4i}= 1160 N/mm, c_{1i}= 2.18 Ns/mm, (i=1,2,3,4). For the linear model the parameters identified are $k_{zi}^{lin} = 987$ N/mm, $c_{zi}^{lin} = 2.52$ Ns/mm. The ability of the two models to predict the foot behavior is quantified in Table 3.

The measurements were performed with pure vertical loading of a foot (see test rig in Fig. 9) and the parameters in the *x*-*y* directions were related to the vertical properties by using a finite element model available at Asko Appliances AB. In the FE model a load was applied to a node vertically and the displacement at the node in vertical direction was registered. Later, a pure lateral load with same magnitude as the vertical one was applied and the lateral displacement was registered. The ratio between the displacements was then used to determine the model parameters in the lateral directions. By using this method it was found out that the foot was 1.5 times stiffer in the *z*-direction than in the *x*- and *y*-directions. The damping properties were scaled with the same proportions. Resulting parameters were $k_{xi}^{lin} = k_{yi}^{lin} = 658$ N/mm, $c_{xi}^{lin} = c_{yi}^{lin} = 1.68$ Ns/mm.

4.3 Model verification and validation

Parameters used for verification and validation of the model

Based on the results of the parameter identification problem solved for the suspension component models the parameters according Tables 5, 6, and 7 were used. The values for center of mass position vector and orientation vectors of axes inertia are given as they are at static equilibrium position. Orientation values are given as sequential rotations around *z*-*x*'-*z*'' with respect to the global axis. Position values are given with respect at the global origin which in the model is located in the center of the bottom plate.

Table 4 Parameter values of the inertial functional components

Part	Param	Value [kg]	Param	Value [kgmm^2]	Param	Value [mm]	Param	Value [deg]
Drum	m_d	6.68	$\boldsymbol{I}_d$	2.1*10^5, 1.9*10^5, 2.2*10^5	$\boldsymbol{x}_d$	0, 79, 438	$\boldsymbol{\theta}_d$	0.0, 0.0, 0.0
Tub system	m_t	35.6	$\boldsymbol{I}_t$	2.3*10^6, 1.7*10^6, 1.9*10^6	$\boldsymbol{x}_t$	1, -32, 403	$\boldsymbol{\theta}_t$	-24.9, -0.7, -0.1
Unbalanced load	m_u	0.3	$\boldsymbol{I}_u$	0, 0, 0	$\boldsymbol{x}_u$	0, -167, 215	$\boldsymbol{\theta}_u$	0, 0, 0
Housing	m_h	26.8	$\boldsymbol{I}_h$	3.0*10^6, 3.1*10^6, 2.4*10^6	$\boldsymbol{x}_h$	2, -80, 348	$\boldsymbol{\theta}_h$	6.2, 1.5, 9.4
Motor rotor	m_m	2.5	$\boldsymbol{I}_m$	3600, 3100, 3600	$\boldsymbol{x}_m$	10, 85, 112	$\boldsymbol{\theta}_m$	0, 0, 0
Strut piston[1]	m_p	0.17	$\boldsymbol{I}_p$	400, 400, 0	$\boldsymbol{x}_p$	-221, 111, 159	$\boldsymbol{\theta}_p$	0.0, 8.9, 0.0
Strut cylinder[1]	m_c	0.19	$\boldsymbol{I}_c$	700, 700, 0	$\boldsymbol{x}_c$	-240, 111, 46	$\boldsymbol{\theta}_c$	0.0, 8.9, -25.5

[1]) All struts have same inertia properties

Table 5 Parameter values of the stiffness functional components

Component	Parameter	Value [N/mm]	Parameter	Value [mm]
Strut spring[1]	k_s	2.9	z_0	110
Stabilizing top spring[2]	k_t	1.5	x_0	134

[1]) All struts have same stiffness properties

[2]) Both springs have same stiffness properties

Table 6 Parameter values of the damping functional components

Component	Parameter	Value [N]	Parameter	Value [Ns/mm]	Parameter	Value [mm/s]
Strut damper left front	F_{01}^h	15.9	C_1^h	0.051	α_1^{sat}	12.5
Strut damper left back	F_{02}^h	18.2	C_2^h	0.061	α_2^{sat}	13.5
Strut damper right front	F_{03}^h	25.2	C_3^h	0.072	α_3^{sat}	14.2
Strut damper right back	F_{04}^h	27.1	C_4^h	0.077	α_4^{sat}	12.1

Table 7 Parameter values of the stiffness damping functional components

Component	Param	Value	Param	Value	Param	Value	Param	Value
Lower bushing[1]	$K^{l}_{x'}$	2 8 Nm/deg	$K^{l}_{y'}$	2.8 Nm/deg	$C^{l}_{x'}$	0.04 Nms/deg	$C^{l}_{y'}$	0.04 Nms/deg
Upper bushing[2]	$K^{u}_{x'}$	2.0 Nm/deg	$K^{u}_{y'}$	2.4 Nm/deg	$C^{u}_{x'}$	0.02 Nms/deg	$C^{u}_{y'}$	0.02 Nms/deg
Foot[3]	k_0	168 N/mm	c_0	33.8 Ns/mm	k_1	-1870 N/mm^2	k_2	13800 N/mm^3
	k_3	-413 N/mm^4	k_4	1160 N/mm	c_1	2.18 Ns/mm		
	k_x^{lin}	658 N/mm	k_y^{lin}	658 N/mm	c_x^{lin}	1.68 Ns/mm	c_y^{lin}	1.68 Ns/mm

[1]) *All upper bushings have the same properties*

[2]) *All lower bushings have the same properties*

[3]) *All feet have the same properties*

In Table 8, all coordinates are given with respect to the global origin which is placed at point O, see Fig. 2.

Table 8 Coordinates of the connection points for struts, stabilizing springs and machine feet

Point	$\mathbf{Q}_{LF}$	$\mathbf{Q}_{LB}$	$\mathbf{Q}_{RF}$	$\mathbf{Q}_{RB}$	$\mathbf{P}_{LF}$	$\mathbf{P}_{LB}$	$\mathbf{P}_{RF}$	$\mathbf{P}_{RB}$
x (mm)	-207	-207	207	207	-249	-249	249	249
y (mm)	-130	111	-130	111	-130	111	-130	111
z (mm)	247	247	247	247	-8	-8	-8	-8
Point	$\mathbf{R}_{LF}$	$\mathbf{R}_{LB}$	$\mathbf{R}_{RF}$	$\mathbf{R}_{RB}$	$\mathbf{S}_{F}$	$\mathbf{S}_{B}$	$\mathbf{T}_{F}$	$\mathbf{T}_{B}$
x (mm)	-260	-260	260	260	0	0	0	0
y (mm)	-206	206	-206	206	-240	256	-69	79
z (mm)	-45	-45	-45	-45	726	734	714	694

Verification of computational model

To be able to trust a computational implementation of a mathematical model a convergence of the numerical solution is necessary. The methodology to achieve is to gradually decrease the error tolerance of the numerical solvers integrator until the change in the results becomes negligible. So, to verify the computational implementation of the washing machine simulations were done with different tolerances. The simulation results for a foot force when using this procedure is shown in Fig. 19.

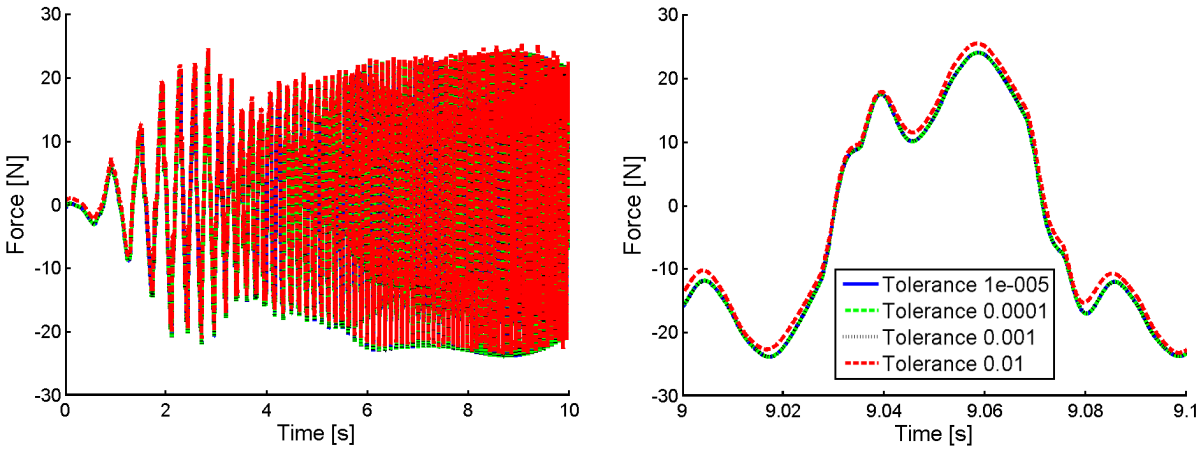

Fig. 19 Vertical force at front left foot at different integrator tolerances

The point of conversion in terms of integrator tolerance was deemed to be 0.001 which with Adams I3 integrator formulation corresponds to a maximum absolute error in a displacement state variable of 1 μm [40]. An integrator tolerance of 0.001 is also the default tolerance in Adams/View.

Validation of computational model

Even though individual experiments on many of the suspension components have been done not all values of the components´ parameters have been determined. Stiffness values at static conditions of the rubber bushings have been determined, but the dynamic properties of the bushings have not been tested with a trustworthy method. To tune the values of the unknown parameters an optimization problem can be formulated problem A. The problem is formulated so that its solution minimizes the RMS-error of the contour function of the model output data and with respect to the experimental data.

The contour (envelope) function used is be described by the algorithm in Fig. 20.

First the signal containing time data points $\mathbf{R}(t,x)$ *is divided into segments corresponding to the frequency of the oscillation at the current instance of time*

For each segment

The maximum[1] *of the signal and the time instance during the segment is stored as point* $\mathbf{P}$

End for

For each stored point $\mathbf{P}$

Calculate the vector $\mathbf{U}_i$ *between the point* $\mathbf{P}_j$ *and the next point* $\mathbf{P}_{j+1}$

For each point $\mathbf{R}_i$ *in the original data between (in time) the stored point* $\mathbf{P}_j$ *and the next stored point* $\mathbf{P}_{j+1}$

Calculate the vector $\mathbf{V}_i$ *between the point* $\mathbf{R}_i$ *and the stored point* $\mathbf{P}_j$

Calculate the projection $\mathbf{V}_{ui}$ *of the vector* $\mathbf{V}_i$ *on* $\mathbf{U}_i$

End for

Find the maximum $\mathbf{V}_{i*}$ *of* $|\mathbf{V}_i-\mathbf{V}_{ui}|$ *on i*

if the projection of ($\mathbf{V}_{i*}-\mathbf{V}_{ui*}$) *on the* $\mathbf{e}_x$ *is > 0 then*[2]

Add $\mathbf{R}_i$ *point to the list of stored points*

end if

End for

1) Minimum for the lower contour
2) < 0 for the lower contour

Fig. 20 Algorithm for the contour function

As an example of the output from the above implementation two functions have been defined according to the following equations

$$y(t) = \sin(t)\sin(2\pi t^2),\ t = [0,10] \tag{21}$$

$$y(t) = \sin(t)\sin(2\pi t^2) + r(t),\ t = [0,10] \tag{22}$$

where *r(t)* is a random number between 0 and 1. The resulting upper and lower contours of the signals are presented in Fig. 21.

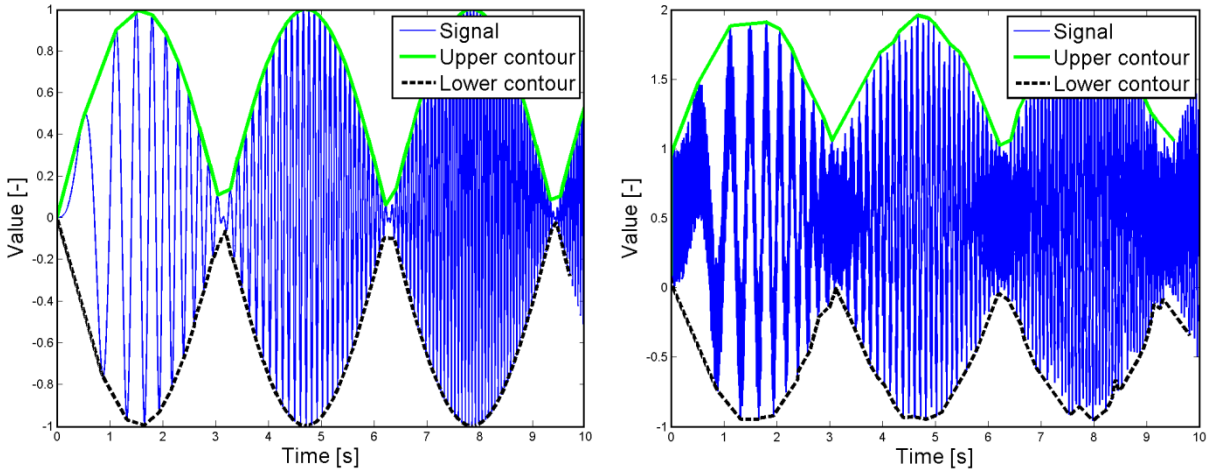

Fig. 21 Signals with varying frequency together with their corresponding contours, a) without noise b) with noise

The parameter identification problem

The problem is stated to find the vector of parameters $\xi = \xi_*$ which satisfies the variational equation

$$E_M = k_d \mathrm{E}_D(\xi_*) + E_F(\xi_*) = \min_{\xi} \left\{ k_d \mathrm{E}_D(\xi) + E_F(\xi) \right\} \tag{23}$$

subject to the differential constraints (16) and initial state (17). In (23) the functions describing prediction errors are defined as follows

$$\mathrm{E}_D(\xi) = \sqrt{\frac{1}{3}\sum_{j=1}^{3} \left(\mathbf{F}\left[\mathbf{y}_{Di}(t,\xi,\mathbf{S}) \right] \right)^2 - \left(\mathbf{F}\left[\mathbf{y}_{Di}^{\exp}(t,\xi,\mathbf{S}) \right] \right)^2} \tag{24}$$

$$\mathrm{E}_F(\xi) = \sqrt{\frac{1}{4}\sum_{j=1}^{4} \left(\mathbf{F}\left[\mathbf{y}_{Fi}(t,\xi,\mathbf{S}) \right] \right)^2 - \left(\mathbf{F}\left[\mathbf{y}_{Fi}^{\exp}(t,\xi,\mathbf{S}) \right] \right)^2} \tag{25}$$

Here **F** is the functional giving the contour (envelope) of the output of the functions $\boldsymbol{y}_{\mathbf{D}}$ and $\boldsymbol{y}_{\mathbf{F}}$, which are the displacement and force outputs, taken from measurements or from simulation data. Due to the difference in magnitude between the force and displacement data a scaling coefficient k_d =0.1 was applied. The outputs are determined by experiments or by solving the initial value problem (16), (17) which is implemented in the Adams model. The vector of varying parameters ξ was set to include the parameters which had not been measured separately in test rigs or taken from trustable sources. It was defined as: $\xi = \left\{ C_{x'}^{l}, C_{y'}^{l}, C_{x'}^{u}, C_{y'}^{u}, K_{x'}^{u}, K_{y'}^{u} \right\}$. The values of the parameters corresponding parameters included in the found solution ξ_* are available in Table 7.

The so called spinning operational scenario (SOS), which is the vector argument **S** in (24) and (25) is constructed from the parameters describing the load configuration and the input spin speed ω(*t*). The selected input speed is corresponding to a part of the imbalance load weighing scheme of the washing machine containing acceleration and deceleration of the drum rotation. The load comprises no balanced load but an unbalance of m_u=0.3 kg placed at the bottom front most position in the drum (see Table 4 for detailed imbalance parameters). By using the results from the optimization, parameters were tuned for better agreement between model with experimental data. The contours of the measurement of the tub motion at position P_{TC} are plotted together with the results of a simulation using the best parameters in Fig. 22. The data show good agreement for the displacement in the *y* and *z*-direction. In the *x*-direction the main behavior is captured by the model but the peak-to-peaks of is wrong by 25%.

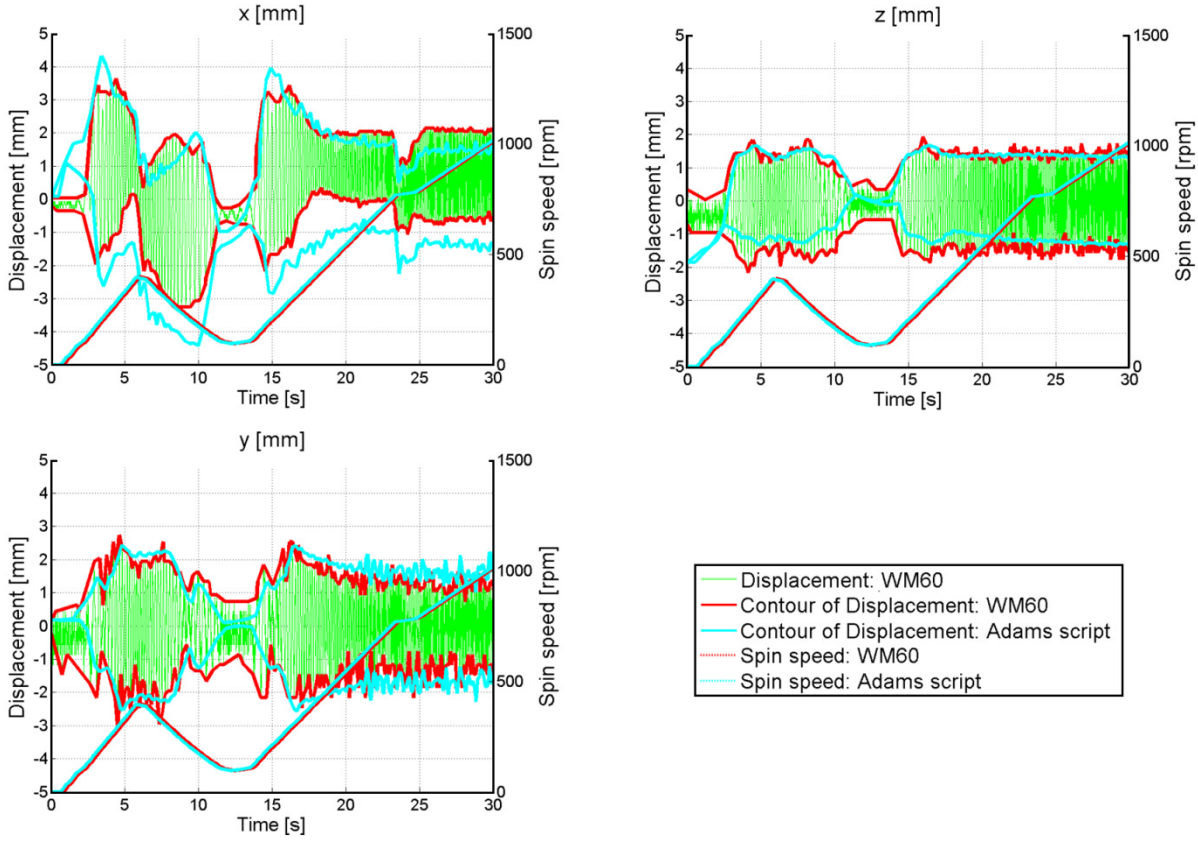

Fig. 22 Experimental and simulation data describing the position of the tub at position PTC.

The total RMS error for the displacement was E_D=2.7 mm. It should be noted that the value corresponds to the sum of the errors over 3 channels and over both contours.

The contours of the vertical reaction forces are plotted in Fig. 23. The total RMS error for the forces, E_F=39 N summarized on four channels. Representation of the data is best at lower speeds. In the range of the data corresponding to spin speeds below 500 rpm the modeled

forces describe the measured data better than at high speed. The modeling is done assuming all bodies as rigid, which seems like an over-simplification when observing the machine. Many modes originating from flexible body motion of the different plates of the housing can be observed by oscillations visible to the eye.

The value of the minimal weighted error between simulation and measurement data was found as $E_M = 6.6$.

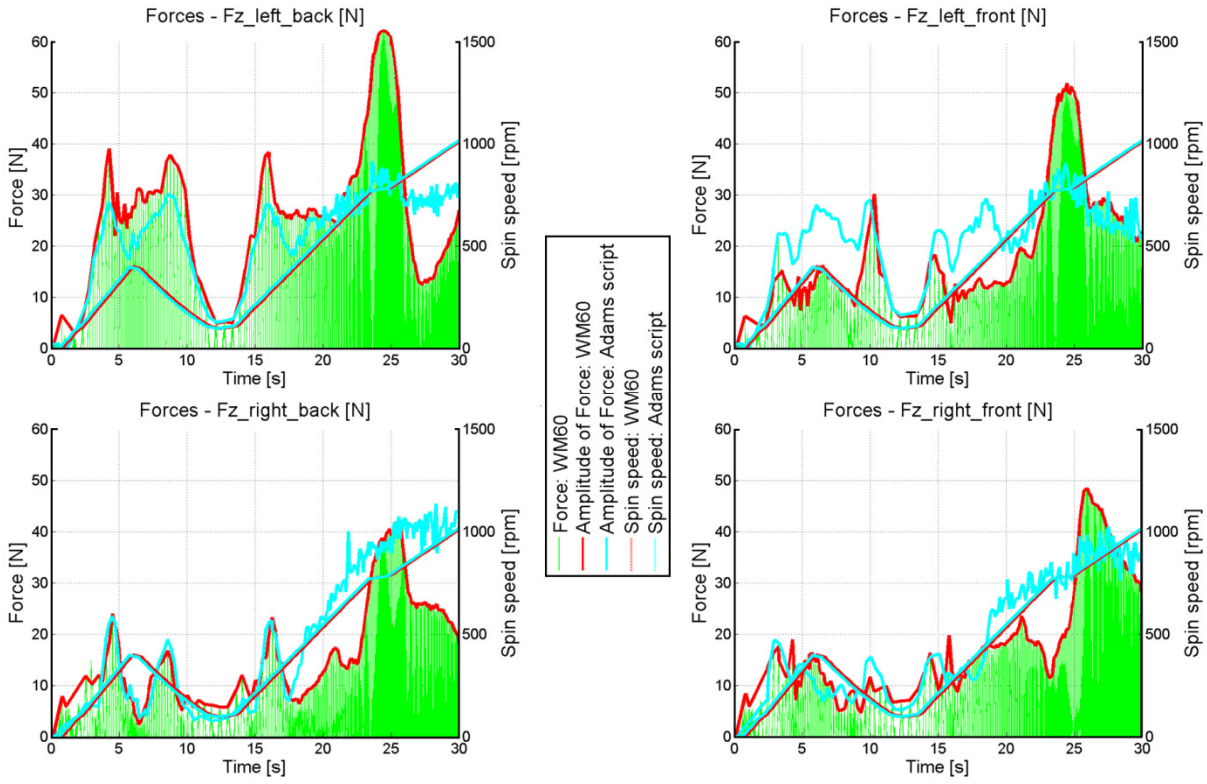

Fig. 23 Experimental and simulation data of vertical transmitted forces at the machine feet

5 Computational model applications

The computational model has been developed with the aim for analysis of vibration dynamics and to optimize the components of the washing machine. With this in mind priority has also been put on time performance in calculation of the dynamics for given inputs. One method to dramatically increase the performance of calculation is parallelization of calculation. If the response of a model is to be calculated on different sets of known parameters, the calculation can be started at once on all parameters of the each set. To accomplish this in the Adams/View environment a cluster controller has been built in Matlab. The controller sends simulation data, via the network, to different ordinary workstation computers running Adams/View. To make this possible several macros and functions have been programmed

Adams/View and in Matlab respectively. In [36] a performance measure of the cluster is presented together with an application of it. All simulations performed in this section have been done through execution on the cluster.

5.1 Vibration dynamics analysis

The outputs of the washing machine model in the scope of the current research project are different characteristics of vibrations, primarily contact forces between the washing machine and surroundings, and kinematics of the tub system. Other signals like forces of constraints and functional components are easily recorded and exported if found useful in the future. Input to the model is the desired rotational speed of the drum as a function of time together with imbalance parameters $\{m_u, \mathbf{I}_u, \mathbf{x}_u, \boldsymbol{\theta}_u\}$.

One important aspect of a dynamical system is the eigenvalues and eigenvectors of the system matrix. These properties are directly coupled to the vibratory characteristics of the system. The linearization of equation (16) performed by Adams/Solver gives the linear equation $\dot{\mathbf{x}} = \mathbf{A}\mathbf{x}$ with the system matrix $\mathbf{A}$. Note that the matrix $\mathbf{A}$ includes the inertia $\mathbf{M}$, stiffness $\mathbf{K}$, and damping $\mathbf{C}$, properties of the system and is defined by

$$\mathbf{A} = \begin{pmatrix} \mathbf{0} & \mathbf{I} \\ -\mathbf{M}^{-1}\mathbf{K} & -\mathbf{M}^{-1}\mathbf{C} \end{pmatrix}$$

For the considered washing machine the matrix $\mathbf{A}$ as well as the representation of the state variables x_1, x_2, x_3,…, x_{24} are presented in appendix A. Coupled to the eigenvalues properties like damping ratios and eigenfrequencies can be calculated.

Depending on the damping present in the system the eigenvalues can be either complex or real valued. In case of a real valued eigenvalue the motion pattern described by the respective eigenvector mode, is overdamped and is not oscillating. Instead it is prescribed by an exponential decay. The case of underdamped mode will correspond to an eigenvalue having a complex part. The mode coupled to such an eigenvalue will correspond to a damped angular frequency described by its complex part. For the pure complex frequency the mode is undamped. In a rotary system gyroscopic forces will affect the eigenfrequencies. It will come in as a reaction torque orthogonal to the spinning axis and to the axis of the applied torque. The gyroscopic moment is a function of the angular frequency of rotation of the drum in the case of the washing machine. It is therefore interesting to analyze what happens with the eigenfrequencies or resonances as the spin speed changes. To make the effect clearer the damping is removed from the system during this study. In Fig. 24 the eigenfrequencies are

plotted with the unit (rpm) against the actual spinning speed at the time which the system is linearized.

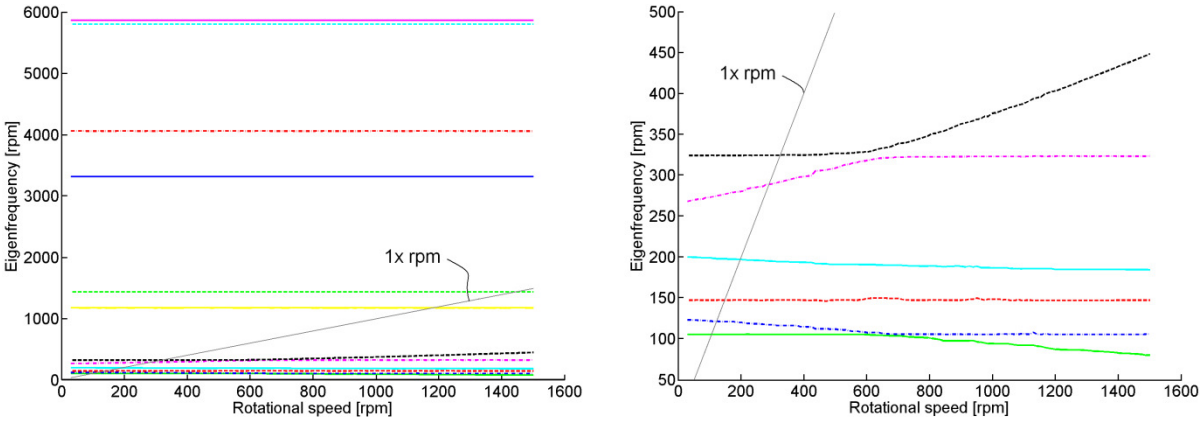

Fig. 24 a) The change of the eigenfrequencies with varying rotational spinning speed, b) only showing the six first eigenfrequencies

It can be seen in that among the six first eigenfrequencies, the ones affected by the rotational spinning of the drum are three to the number. To identify the mode shapes of the washing machine system the model in Adams is set to animate the motion related to the eigenvectors. As motions of the washing machine are complex shaped the positions, during an oscillating in a mode, are superimposed on each other to illustrate a trace of the motion. The motion magnitude is scaled so that it becomes clearly visible.

In Fig. 25 the six first mode shapes are shown for the rigid body system linearized at its equilibrium position at t=0 with spin speed $\omega(0)$=0. The modes are ordered from the left to right and top to bottom. The first mode can be described as a translation of the tub in the x-direction with a slight rotation about the y-axis, the second by an inverse pendular motion around a point below the tub, the third by a translation of the tub in the vertical direction, the forth by a rotation around the vertical axis of the center of mass of all the parts suspended by the struts combined, the fifth by a pendular motion around a point slightly above the tub center, and the sixth by a rotational motion of the tub with around a point slightly above the drum rotation axis. It is almost a rotational motion around this axis. In Fig. 25 it can be seen that the first 6 modes only involves motion of the suspended tub. The bottom plate representing the housing remains still. The probable reason is that the tub suspension is much softer than the feet of the machine which suspend the housing.

Fig. 25 Trail animation of the first six eigenmodes with corresponding frequencies

A dynamic model can be studied in many ways using different functions which describe aspects in terms of dynamics response. The developed washing machine model has several outputs i.e. is of multi-output type, meaning that the response of an input can be studied at each output separately. The outputs are of different types and measures different characteristics which consequently can be used to different aspects of the performance of a washing machine. Examples of outputs are the following: 1) The motion of the tub relatively to the housing. For example, a measurement of motion can be taken between different positions. One is at the center of mass of the suspended tub-unit. Other positions are at critical locations where there lies a risk for collision during spinning. Maximization of capacity leads to smaller and smaller margins between tub and housing. 2) The transmitted forces between the machine and the structure it stands on. The levels of the forces are naturally interesting to

study for vibration isolation purposes. But, also the ratio between lateral and vertical forces are interesting as this ratio is coupled to the friction coefficient of the foot. To make the machine stand still and not walk around, the friction between the supporting structure and the machine must be sufficiently high. 3) The eigenvalues of the washing machine system will determine at which excitation frequencies extra high vibration levels are to be expected. During spinning it is important to pass by these frequencies quickly and also not to design a spinning speed plateau in the proximity of such frequency.

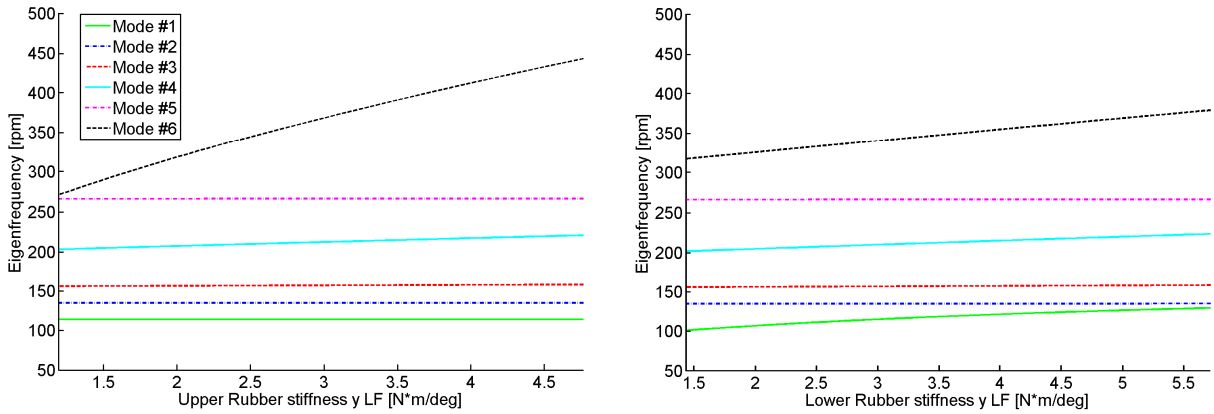

Fig. 26 Influence of upper $K^u_{y'}$, and lower $K^l_{y'}$, bushing stiffness on eigenfrequencies at static equilibrium

Variations of the parameters around their current value have been performed and the results show that the stiffnesses of the bushings have significant influences on the eigenfrequencies corresponding to modes which involve large displacement of the respective rubber component, see Fig. 26. It can be concluded that the frequency of the first mode is affected by the lower bushing stiffness around *y*-axis. The lower bushing here counteracts the translation whilst the piston at the same angle with respect to the upper bushing, Fig. 25. The sixth mode is strongly affected by both bushing stiffness values around the *y*-axis. For the fourth a slight change can be observed towards higher values of frequency for stiffer bushing values. The frequencies of remaining modes remain unchanged with this variation of the bushing stiffness, see Fig. 26.

Note that the linearization and eigenvalue calculations were done with all damping set to zero to study the eigenfrequencies only. But for evaluation of the performance of the machine at critical speeds, the modal damping should be known. The damping matrix $\mathbf{C}$ represents the various dissipation mechanisms in a vibrating system. These mechanisms are usually poorly known. One of the most popular hypotheses about these mechanisms is the assumption that the damping matrix is represented as a linear function of inertia and stiffness matrices with two weighting coefficients. The coefficients are selected to fit the considered system and the damping is called Rayleigh damping.

The damping matrix $\mathbf{C}$ can be also determined using estimated modal damping factors. In this procedure, the undamped eigenvalues and modes of the system must be solved from $(\mathbf{K}-\omega_i^2\mathbf{M})\boldsymbol{\varphi}_i=0$, where ω_i is the angular frequency, $\boldsymbol{\varphi}_i$ is the mode shape vector of mode i, $\mathbf{K}$ and $\mathbf{M}$ are stiffness and mass matrices of the system. Then the mode shape matrix of the *n* modes $\boldsymbol{\Phi}$ can be constructed using the solved mode shape vectors as $\boldsymbol{\Phi}=[\boldsymbol{\varphi}_1,\boldsymbol{\varphi}_2,\boldsymbol{\varphi}_3,...,\boldsymbol{\varphi}_n]$, where the modes $\boldsymbol{\varphi}_i$ are normalized with respect to the mass matrix as follows $\boldsymbol{\Phi}^T\mathbf{M}\boldsymbol{\Phi}=\mathbf{I}$. Here $\mathbf{I}$ is the unit matrix. The modal damping matrix $\mathbf{C}_m$ is a diagonal matrix, the elements of which can be calculated as $c_i=2\xi_i\omega_i$, where ξ_i is the modal damping factor of mode i. Finally, a full damping matrix can be obtained from the modal damping matrix by using the inverse transformation as follows $\mathbf{C}=\left(\boldsymbol{\Phi}^T\right)^{-1}\mathbf{C}_m\boldsymbol{\Phi}^{-1}$.

To see the effect of different suspension parameters upon the transmitted force, a dynamic objective is defined according to (26), and on the relative motion of the tub towards the housing at a interesting point $p=p_2$ as defined by (27)

$$F_D=\sum_{i=1}^{4}\sqrt{\frac{1}{T}\int_0^T\left(F_i^z(t)-F_i^z(0)\right)^2dt} \tag{26}$$

$$F_{Kp}=\max_t\left(\Delta X_p(t)\right) \tag{27}$$

Where $X_p(t)$ is the motion in the direction towards the nearest housing structure. Here $X_p(t)$, was the motion of a point on the front top of the tub towards the housing in *y*-direction.

Constituting the spinning operational scenario used for the parameter study is an imbalance load of 0.5 kg placed at the front of the drum together with a ramp in speed starting from 0 rpm and reaching 1000 rpm in 20 seconds.

In Fig. 27, the responses of the functions F_{Kp} and F_D respectively when the upper and lower bushing stiffness are varied around their default value according to Table 7 . One parameter at a time was selected for variation

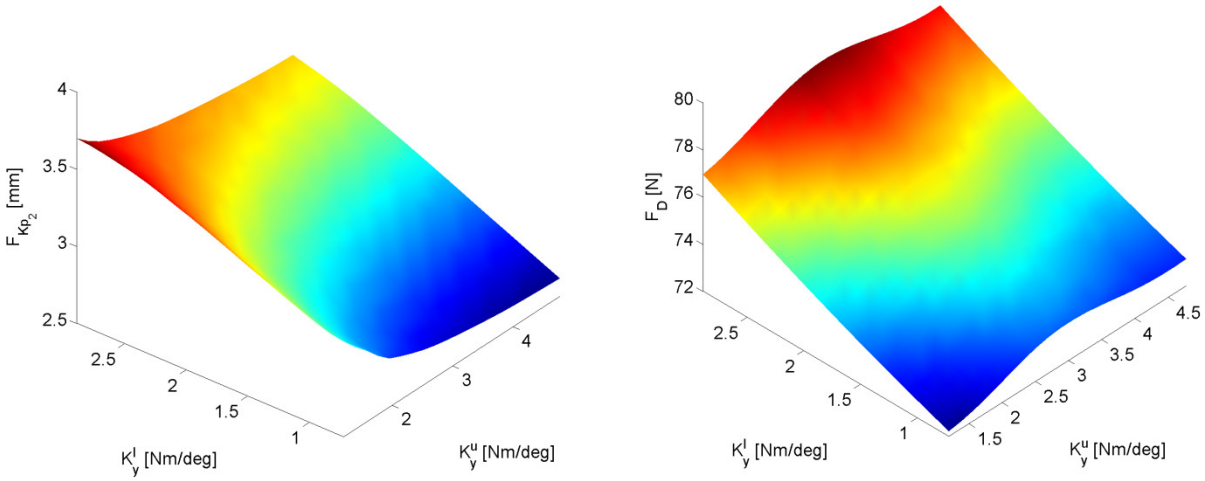

Fig. 27 a) Kinematic and b) dynamic responses due to variations of rubber parameters

Variation of the rubber parameters towards stiffer values does not always results in less movement of the tub. Increased stiffness around the *y*-axis for the lower bushing will for example lead to increased motion of the tub. With stiffer bushings at the lower end more motion is expected at the top end of the tub. In order to make the top move less also the stiffness of the upper bushings needs to be adjusted upwards. In the case of the current example even making both bushings stiffer at the same time did not reduce the motion amplitude as the measurement direction selected point p_2 corresponds to a direction orthogonal to the axis around which the stiffness was changed. Close monitoring of all interesting directions is required to ensure that the right effect is achieved when parameters are changed. A criteria used for monitoring motion in critical directions is given in [32].

5.2 Counterbalancing

The main part of vibrations in washing machines is caused by a poorly distributed wash load around the circumference of the drum. Other reasons can be poor centricity or other asymmetries of the manufactured parts. Experiments have shown that manufacturing errors can play a role and is generally not negligible in a production machine. The imbalance can be of different types; static and dynamic. Static imbalance means that the position of the combined center of mass of the rotating system (drum and imbalance) is not located on the axis of rotation of the drum, but that one principal axis of inertia remains parallel to it, see Fig. 28a. Pure dynamic imbalance does not change the position of center of mass of the system but will result in that none of the principal axis of inertia no longer is parallel to the spinning axis, see Fig. 28b.

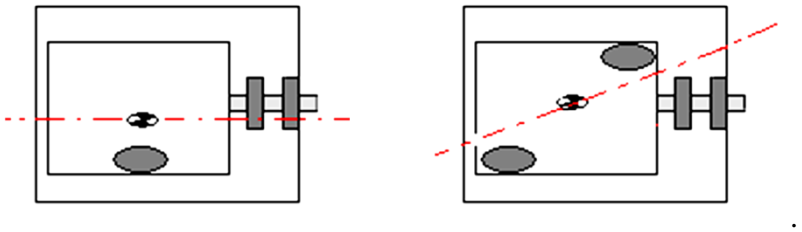

Fig. 28 Sketches showing center of mass and inertia axes at: a) static imbalance and b) dynamic couple imbalance

In reality the most probable case is that both static and dynamic imbalances are present at the same time. Together they produce a two plane imbalance, also referred to as a static-dynamic imbalance. Pure dynamic imbalance is also referred to as dynamic couple imbalance. To counteract a general static-dynamic imbalance balancing in two planes is necessary, as indicated by the name. If only static imbalance is present then counterbalancing is necessary in only one plane, being the plane as the imbalance is present in and which is perpendicular to the spinning axis.

Several strategies to counterbalance the unbalanced load have been proposed. Some are active solutions which require external sensing and control to position counteracting solid masses. Examples of such are described in [3] and [10]. Other solutions involve translation of the spinning axis relative to the drum [11, 12, 13] by using a mechanism for control of the eccentricity. Ideas on using liquid (water) which is easily accessible in washing machines to position the total center of mass has also been discussed and studied in [11]. There are also passive solutions to the problem of counterbalancing. With passive solutions it is meant technology which does not need external control stimuli, instead the positioning is done using the circulatory forces coming from rotation of a counterweight. Passive counterbalancing can be done with liquid like in the Leblanc balancer in [14] and [2] or derivations [15]. It can also be done with solid masses. In [2] a concept based on an elastically suspended solid ring is presented, but typically the masses consist of balls of stainless steel [16] or with pendulums or sliders like in [19]. If done with multiple solid pendulums, balls or sliders the functional principle can be illustrated like done in Fig. 29. The total system will at a steady state overcritical speed rotate around the effective center of mass marked by a ring in the figure. The balancing masses will experience a centrifugal force driving them away from this point. At the same time the balance ring around which the masses travel, marked by a dotted circle will give a reaction force perpendicular to the trajectory, see Fig. 29a (Phase I). The resulting forces on the two balancing masses will move the masses to a new position Fig. 29b (Phase 2). When the balancing masses have reached such a position where the resulting center of

mass coincides with the rotational axis the circulatory forces and reaction forces become parallel and does not affect the ball along the trajectory any further Fig. 29c (Phase III).

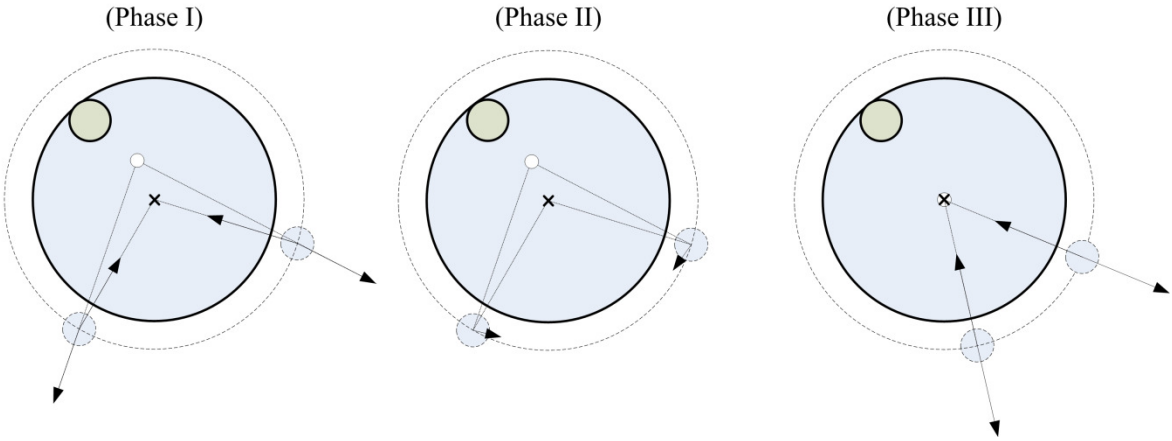

Fig. 29 Principle of passive balancing using two solid masses. The total center of mass of the rotating system is marked by a ring and the rotating axis is marked by a cross

As stated earlier, if the balancing ring and an unbalanced mass are placed in the same plane at the same location in *y*-direction the effect of the imbalance can be canceled out completely. However as it is seldom that the position of the imbalance can be controlled, it can very well end up in the front end or at the back end of the machine causing poor functionality of the automatic balancer.

The presented Adams model has been extended to model washing machine dynamics for a washing machine having two counterbalancing devices capable of reducing imbalances independently of location inside the drum. The devices can be controlled easily by a graphical user interface in which some properties related to the devices can be edited. The location of the respective device along the y-axis of the machine, the balance ball masses, and imbalance levels are example of parameterized features. Each counterbalancing device comprises 5 ball-shaped masses, each of mass m_{BB}=0.1 kg, I_{BB}=9 kgmm^2, which slide in along a circular trajectory with the radius R_{BB}=300 mm in a plane perpendicular to the rotary axis. A schematic representation of the imbalance and balancing system in one plane is depicted in Fig. 30. The balls are kept in the trajectory by using a revolute joint placed between each ball and the drum. In reality the device would consist of some type of housing in which the masses would roll or slide. The housing in its turn would then be attached to the drum. With the two balancing devices the model gets 10 degrees of freedom extra and hence a little more computational demanding, especially when the motions of the balls are large.

Details on how to write analytical the equations for the dynamics of rigid rotors having two passive balancing devices are for example available in [17] and [18]. In the latter effects of

different geometrical defects such as eccentricity and ellipticity on the performance of the balancing mechanism

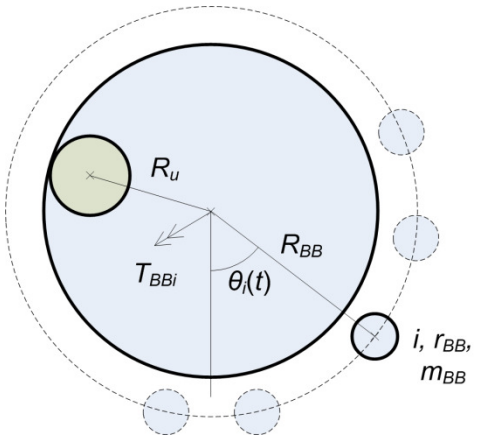

Fig. 30 An example of the arrangement of the balance balls during the approaching to dynamic equilibrium

The center of the circular trajectory is placed on the drum axis. The masses interact with each other by a Hertz contact which, for two equal spheres with Young's modulus E and Poisson's ratio ν, can be written [41] according to

$$F_H = \frac{4}{3} E^* \sqrt{R^* d^3} \tag{28}$$

where the balance ball spheres have radius r_{BB} and the indentation depth is d.

$$E^* = \frac{E}{2(1-\nu^2)},\ R^* = \frac{r_{BB}}{2}, \tag{29}$$

Naturally only balls next to each other can come in physical contact need have an interaction force specified. The Hertz contacts between all the balls which could come in contact are implemented by using 10 contact elements.

During spinning at steady state conditions with a constant imbalance when the balancing is in operation the balls need to rotate around the spinning axis with the same angular velocity as the drum. To accelerate the balls up to spinning speed but still allow relative motion between the drum and the balls N_T=10 viscous torques are added. In some applications, for example oil can be used [16] as a medium to fill up the space between the balls to transfer forces to the balls. The modeled balancer is not of this type; instead it is a fluid less balancer where the balls are greased to increase their rolling resistance to the ball housing which moves with the drum. This arrangement can be treated with fluid dynamic expressions for the ball driving force for a close and detailed study of the interaction between the balls and their housing. But in the current implementation a simplification has been made. It is assumed that the driving forces of the automatic balancing device can be modeled by torque proportional to the

difference in angular velocity between the drum and respective ball. If the drum is rotating with the angular velocity $\omega(t)$ the torques affecting the balls along the circular trajectory can be written

$$T_{Bi}(t) = C_B\left(\omega(t) - \dot{\theta}_i^{ball}(t)\right) \; i = 1,2,3,...,N_T \tag{30}$$

where the angular velocity $\dot{\theta}_i^{ball}(t)$ of ball i with respect to the tub around an axis with coincides with the drum spinning axis. The constant C_B shall be chosen in such a way that the response time of the device to a change in spinning speed or imbalance magnitude is minimized and so that a robust solution is given. To study the sensitivity of this selection, a parameter study has been executed.

To counteract the imbalance regardless of its location inside the drum two balancing devices have been added to the Adams model of a particular machine at the ends of the drum, i.e. d_{RB}=150 mm according to the Fig. 31a.

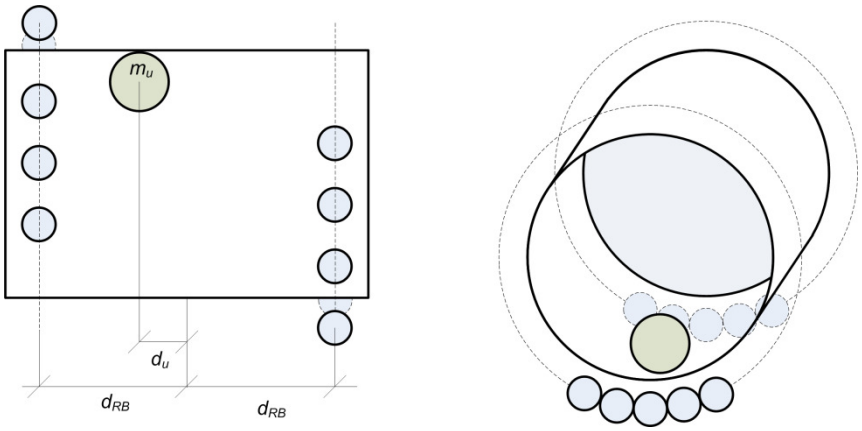

Fig. 31 Arrangement of two balancing devices connected to the drum a) during operation (not counterbalancing) b) at starting conditions of the simulation

Simulations have been run with m_u=0.5 kg of imbalance placed at the distance R_u=252 mm from the drum rotational axis and at d_u=136 mm from the center of the drum while varying the coefficient of viscous torque. Also a simulation has been run with no balancing rings attached to the system. As a measure for comparison the motion of the center of mass of the rotating system (including balancing balls and unbalance) is plotted in the x-, y- and z-directions. Some results of the simulations are available in Fig. 32. The rotational angular velocity of the spinning operation scenario used was a linearly increasing with a gradient 80 rpm/s from 0 rpm up to 800 rpm in counterclockwise direction followed by constant spinning at this velocity for 5 seconds. At start of the simulation all balance balls were placed at their

lowest possible position of their respective constraining circular trajectory and the drum rotated in such a way that the imbalance was at its the lowest position (see Fig. 31b).

In [17] the performance and the rapidness of the counterbalancing mechanism are shown to be dependent on the viscous parameter C_B. To study the influence of this parameter for the current setup a sensitivity analysis was performed using the developed Adams model. The parameter was varied between 1 Nms/rad and 200 Nms/rad with 300 steps and the response in the form of peak-to-peak of the motion of the center of mass in the translational directions was studied.

The time history of translational motion from two simulations with different viscous coefficient C_B are visualized in the plots a-c in Fig. 32 together with the motion of the tub system with no balance ball mechanism attached.

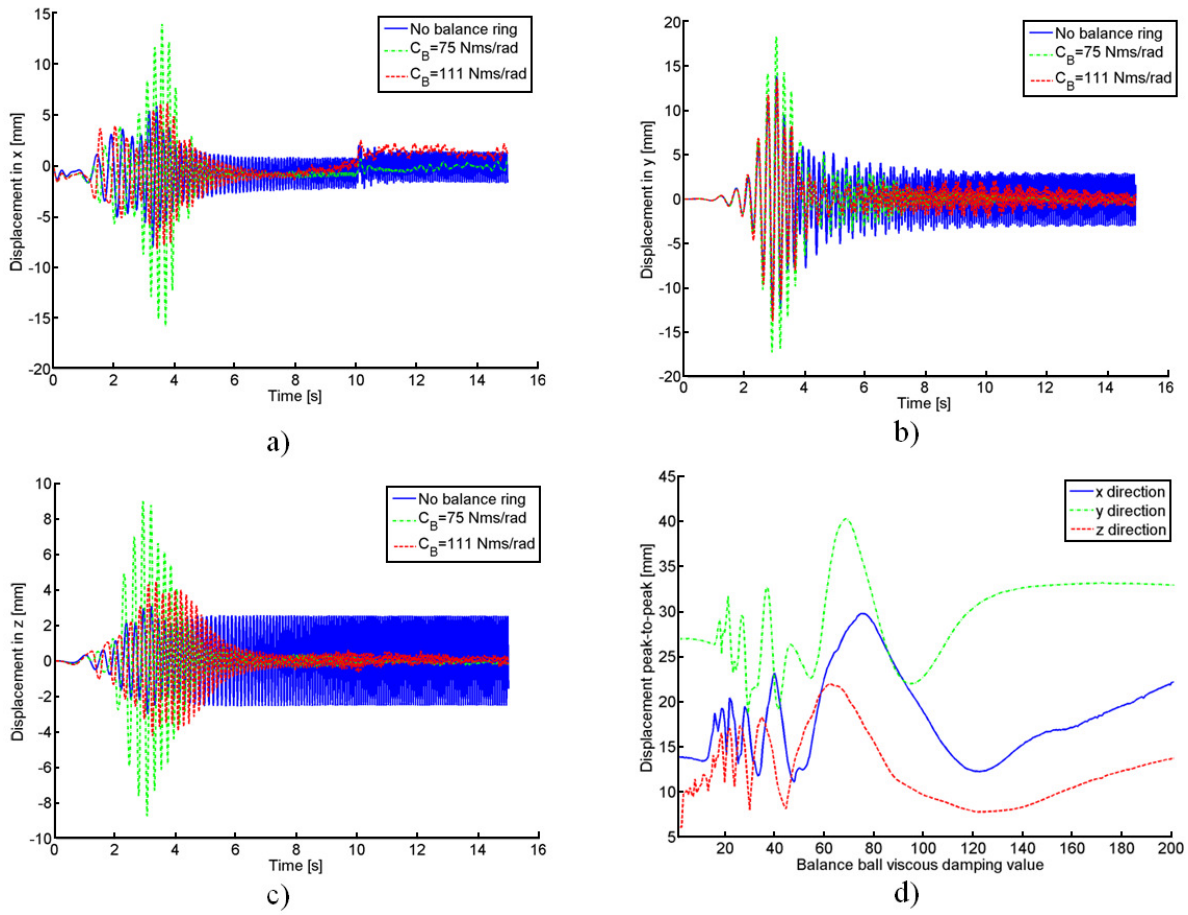

Fig. 32 Motion in of the center of mass of the tub in a) x-direction, b) y-direction, c) y-direction, d) peak to peak values for different viscous coefficient C_B

From the plots a-c in Fig. 32 it can be seen that above a certain rotation speed of the drum system, where the balance balls have positioned themselves, a big reduction of the amplitude

of vibration is possible. However during the ramp spin-up there is bigger motion of the tub with the balancing device than without it for most values of the viscous coefficient C_B. The step in the x-direction at t=10 s comes from the change in the driving torque when reaching the constant part in the spinning velocity scheme. In Fig. 32d several local maxima in respective directions are visible. Each of these maxima corresponds to a value of the viscous coefficient of such value that the viscous torque pushes the balance balls in such way that they are for a short instance of time moving synchronously with the imbalance and that the angle between the imbalance and the center of mass of the balance balls of the two mechanisms are zero. For each local minimum the corresponding angle is as near as possible to the one of their respective counterbalancing position. An important conclusion which should be drawn from the simulation is that the performance of the mechanism is sensitive to the value of the viscous coefficient if it is small. An implementation with a viscous coefficient C_B>80 could be considered more robust with respect to absolute changes of its value as the peak to peak motion is less sensitive to small changes here. There are several reasons to a possible discrepancy between the designed value and the actual value inside a physical device. For example manufacturing tolerances and also aging of components might effect of the balancing ring performance through the viscosity parameter, if this is not taken care of. Another conclusion that could be drawn from the simulations is that the mechanism is quicker if the value of C_B is small, which is a statement confirming the conclusions in [17].

Noted about the passively controlled automatic balancing mechanism described in this chapter should be that no solution to the kinematics problem, i.e. minimization of the tub maximum motion, has been found with the model used. The mechanism is begins to work above certain critical speeds of the tub system and it is when the drum speed is passing these speeds that the maximum motion occurs. The way that the motion of the drum is transferred to the balls is of course of importance to these conclusions, and other models for the ball driving force than the viscous torque of (30) could lead to other conclusions. Nevertheless, the existence of this problem is confirmed by for example [19] where the balance ball motion (relative to the drum motion) is activated only above a certain speed. There are also methods which suggest that the balls of the automatic balancer can be made to counterbalance even at subcritical speed by controlling the motor speed and using gravity to position the balls [42].

The dynamics problem, i.e. minimization of transmitted forces to hosting the structure (e.g. floor), is treated very well if the mass of the unbalanced load is within the capacity range of the device. It could be possible to, with the help of such a device, to reduce the importance of

the dynamics cost function, e.g. (26), in the formulation of the optimization problem for the vibration dynamics in washing machines.

6 Conclusions

The development of high speed spinning washing machines is a great challenge. In the water extraction process, the drum starts rotation and this gives rise to significant centrifugal imbalance forces and imbalanced rotation of the laundry mass. This results in vibration and shaking. By elimination of such vibrations it will be possible to design more silent washing machines for higher wash loads within the same housing dimensions.

In this paper a multibody model of a commercial frontloaded washing machine which has been built using a theoretical-experimental methodology has been presented. The experimentally validated models of functional components have been incorporated into a computational multibody systems model built in MSC.Software/Adams to enable use with an Adams-Matlab interface for clustered simulation and optimization. In the models CAD drawings available from Asko Appliances AB were used giving accurate mass and geometry data of the machine for the simulations.

A full-scale test rig for horizontal-axis washing machines comprising sensors measuring transmitted force of the machine, accelerations and movement of the container and rotational speed of the drum, were built for validation of developed models. Comparisons of obtained results from simulations with measurements show good agreement of drum movement and agreement on level of force output under at low rotational speed under the tested conditions.

A test rig built together with Asko Appliances AB has been used for experimental study of force-displacement characteristics of dampers. Another test rig has been used for measurements on the dynamic response of the machine foot in vertical direction. By using the different test rigs and optimization routines, estimation of the parameters of several damper and foot models has been done successfully. The different models of the strut friction damper component show relative force prediction error down to 8.5% and relative energy dissipation error down to 5%. The best of the found models for foot dynamics show relative prediction errors of 14.6% and 5.6 % respectively.

The developed models and the test rigs have been successfully used for dynamic analysis (eigenfrequencies, eigenmodes, force transmission) and kinematic analysis (drum motion) of a washing machine during spinning. Numerical simulations have also shown the important role in quality of performance of suspension systems in washing machines dynamics that the suspension structural parameters play.

The model has been developed to make it possible to analyze dynamics and vibrations of frontloaded washing machines and can be used to solve several optimization problems for washing machines both with conventional passive suspension as well as with active suspension systems. In this paper the model was used to show the feasibility of a two plane automatic balancing device for vibration reduction. Parametric studies were done on one of the critical parameters, the modeled viscous ball-driving force, of the device to show sensitivity of performance. The limit C_B>80 was determined as lower limit for robust solutions.

Acknowledgements

This work was supported financially by Asko Appliances AB, Vara, Sweden.

The authors wish to thank to Peder Bengtsson, Anders Eriksson, Patrik Jansson, Anders Sahlén and Marcus Person, all working at above mentioned company, for their support and ideas during the project within which this paper was written.

References

1. Conrad, D.C., Soedel, W.: On the problem of oscillatory walk of automatic washing machines, Journal of Sound and Vibration, 188(3), 290-203 (1995)
2. Conrad, D.C.: The fundamentals of automatic washing machine design based upon dynamic constraints, Dissertation, Purdue University, ISBN 9780591345728 (1994)
3. Papadopoulos, E., Papadimitriou, I.: Modeling, Design and control of a portable washing machine during the spinning cycle, Proceedings of the 2001 IEEE/ASME International Conference on Advanced Intelligent Mechatronics Systems (AIM 2001), 899-904, (2001)
4. Türkay, O. S., Sümer, I. T., Tugcu, A. K., Kiray, B.: Modeling and experimental assessment of suspension dynamics of a horizontal-axis washing machine, Journal of Vibration and Acoustics, 120(2), 534-543, (1998)
5. Lim, H. T., Jeong, W. B., Kim, K. J.: Dynamic modeling and analysis of drum-type washing machine, International Journal of Precision Engineering and Manufacturing, 11(3), 407-417 (2010)
6. Donida, F., Ferretti, G., Schiavo, F. : Modelling and simulation of a washing machine, Proceedings of the 50th International Anipla Congress Roma, November 14-15, 2006
7. Yoo, W.S , Kim, K. N., Kim, H. W., Sohn, J. H.: Developments of multibody system dynamics computer simulations and experiments, Journal of Multibody System Dynamics, 18(1), 35-58, (2007)
8. Agnani, A., Cannella, F., Martarelli, M., Merloni, G. Tomasini, E. P.: Dynamic characterization of a washing machine: numerical multi-body analysis and experimental validation, IMAC-XXVI Conference and Exposition on Structural Dynamics, Orlando, Florida, USA, February 4-7, 2008
9. Koizumi,T, Tsujiuchi, N., Matsumoto, S.: Noise prediction of a washing machine considering panel vibration, IMAC-XXVI Conference and Exposition on Structural Dynamics, Orlando, Florida, USA, February 4-7, 2008

10. Hällsås, M.: Design of active balancing systems to offset the imbalance in washing machines, Master's Thesis no. 2007:21, ISSN:1652-8557, Chalmers University of Technology (2007)
11. Ermund, F., Ermund, M.: Design and modeling of an active balancing device for washing machines, Master's Thesis no. 2006:76, ISSN:1652-8557, Chalmers University of Technology (2006)
12. Johansson, T., Kvist, M.: Active balancing control for washing machines, Master's Thesis no. 2007:45, ISSN:1652-8557, Chalmers University of Technology (2007)
13. AB Electrolux: Method and arrangement for balancing of a load supporting device, International patent (PCT) publication number WO 98/48096 (1998)
14. Bae, S., Lee, J. M., Kang, Y. J, Kang, J. S., Yun, R. J.: Dynamic analysis of an automatic washing machine with a hydraulic balancer, Journal of Sound and Vibration, 257(1), 3-18 (2002)
15. Sonoda, Y., Yamamoto, H., Yokoi, Y.: Development of the vibration control system "G-Fall balancer" for a drum type Washer/Dryer, Proceedings of the 2003 IEEE/ASME International conference on Advanced Intelligent Mechatronics, International Conference Center, Port Island, Kobe, Japan, July 20-24, 2003
16. Lindell, H., Thuvesen, D.: Automatisk balansering av roterande maskiner, Mölndal, Sweden, ISBN: 992-508205-6 (1997)
17. Sperling, L., Ryzhik, B., Linz C. H.,and H. Duckstein, H.: Simulation of two-plane automatic balancing of a rigid rotor, Journal of Mathematics and computers in simulation, 58(4-6), 351-365 (2002)
18. Olsson, K.O.: Limits for the use of auto-balancing, International Journal of Rotating Machinery, 10(3), 221-226 (2004)
19. Juhlin, S. G.: Arrangement for balancing of a body rotatable about an axis, United States Patent number 5813253, published Sept 29, 1998
20. Kamath,G. M., Hurt, M. K., Wereley, N. M.: Analysis and testing of Bingham plastic behavior in semi-active electrorheological fluid dampers, Smart Materials and Structures, 5(5), 576-590 (1996)
21. Berger, E. J.: Friction modeling for dynamic system simulation, Applied Mechanics Reviews, 55(6), 535-77, 2002
22. Nygårds, T., Berbyuk, V.: Dynamics of washing machines: MBS modeling and experimental validation, Proceedings of the Multibody Dynamics 2007, ECCOMAS Thematic Conference, Milano, Italy, June 25–28, 2007
23. Havsin function, Adams/View R3 and Adams/Solver R3 documentation, MSC. Software, 2008
24. Ikhouane, F., Mañosa, V., Rodellar, J. : Dynamic properties of the hysteretic Bouc-Wen model, Systems & Control Letters, 56(3), 197-205 (2007)
25. Kang, D.W, Jung, S.W., Ok, J.K, Nho, G.H , Yoo, W.S., "Application Of A Bouc-Wen Model For A Frequency Dependent Nonlinear Hysteretic Friction Damper", Journal of Mechanical Science and Technology, 24(6), 1311-1317 (2010)
26. Ryu, J.C., Nho, G.H., Chung, B.S, Lee, J.H, Jung, S.W, Yoo, W.S, Suggestion Of MSTV (modified Stick Transition Velocity) Model For Hysteretic Damping Mechanism", Journal of Mechanical Science And Technology, 22(7), 1305-1312 (2008)
27. Kim, H. J., Yoo, W. S., Ok, J. K., Kang, D. W.: Parameter identification of damping models in multibody dynamic simulation of mechanical systems. Journal of Multibody System Dynamics, 22(4), 383–398, 2009
28. Suspa Website: "Suspa.com - RD 18 FL" http://www.suspa.com/index.php?id=786 (Accessed January 26 2010)

29. Aweco Appliance Systems webpage, http://www.aweco.de. (Accessed February 1 2010).
30. Hwaxia Li, Wan-Suk Yoo, "Hydraulic Mound Design For A Drum-type Washing Machine Imeche, J. Multibody System Dynamics, Proceedings of the Institution of mechanical Engineeers, Part K: Journal of multi-Body Dynamics, 225(2), 167-178, 2011
31. Vasić, V. S., Lazarević, M.P: Standard Industrial Guideline for Mechatronic Product Design, Faculty of Mechanical Engineering Transactions, 36, 103–108, Faculty of Mechanical Engineering, University Belgrade, Serbia (2008)
32. Nygårds, T., Berbyuk, V., Sahlén A.: Modeling and optimization of washing machine vibration dynamics, Proceedings of the 9th International Conference on Motion and Vibration Control (MOVIC 2008), Technische Universität München, Munich, Germany, September 15-18, 2008
33. Kvist, M., Nygårds, T., Berbyuk, V.: Simulering av fördjupad tvättmaskin. Internal report, Mechanical systems Group, Division of dynamics, Applied Mechanics, Chalmers University of technology, 2007
34. Merediz, A.: Modeling of dehydration process in controlled spinning of washing machines, Master's Thesis no. 2009:33, ISSN:1652-8557, Chalmers University of Technology (2009)
35. Mahmud, A., Cuellar, E.: Optimization of load distribution in washing machines using bio-inspired computational methods, Master's Thesis no. 2010:55, ISSN:1652-8557, Chalmers University of Technology (2010)
36. Nygårds, T., Berbyuk, V.: An Adams/View-Matlab environment for clustered optimization of washing machines, ,Proceedings of the 22nd Nordic Seminar on Computational Mechanics (NSCM), DCE Technical Memorandum No. 11, ISBN 1901-7278, Aalborg University, Aalborg, Denmark, October 22-23, 2009
37. Yarmohamadi,H., Berbyuk,V. Computational model of conventional engine mounts for commercial vehicles: validation and application Journal of Vehicle System Dynamics, 49(5), 761–787, 2011
38. Carvalho, M., Ambrósio, J. Identification of multibody vehicle model for crash analysis using an optimization methodology, Journal of Multibody System Dynamics, 24, 325–345, 2010
39. Vyasarayani, C. P., Uchida, T., Carvalho, A., McPhee, J. Parameter identification in dynamic systems using the homotopy optimization approach, Journal of Multibody System Dynamics, 26, 411–424, 2011
40. Integrator statement, Adams/View R3 and Adams/Solver R3 documentation, MSC. Software, 2008
41. Flügge, W.: Handbook of engineering mechanics, First Edition, section 42-2, McGraw-Hill Book Company, New York, USA, ISBN 0070213925 (1962)
42. Jonsson, J., Lindell, H.: Method for pre-balancing a rotating drum having a temporarily shifting unbalance, United States Patent number 6295678, Published October 2, 2001

Appendix A

In $\dot{\mathbf{x}} = \mathbf{A}\mathbf{x}$, where $\mathbf{x} = [x_1, x_2, x_3, ..., x_{24}]^T$

$$\mathbf{A} = \left(\begin{array}{cccccccccccc|c} \multicolumn{12}{c|}{\mathbf{0}} & \mathbf{I} \\ \hline -503 & 181 & 63 & -2388 & -4280 & 695 & 3396 & 17812 & 315 & 224 & 68 & 1743 & \\ 264 & -525 & 104 & 928 & -46 & -981 & 42 & 1847 & 54 & -261 & -110 & 24 & \\ 1 & -3 & 744 & 1456 & 58 & 1473 & 56 & -5 & 4 & -1 & 131 & -46 & \\ -149 & 312 & 1010 & -270925 & -7743 & -88075 & -10020 & -19607 & -208 & 191 & -158 & 21866 & \\ 467 & -143 & 71 & 34873 & -94015 & 32281 & -20331 & 117030 & -254 & -105 & -38 & 8776 & \\ 198 & -315 & 1153 & -88168 & -10392 & -272726 & -7563 & 20543 & 205 & -153 & -307 & 23244 & \mathbf{0} \\ 68 & 138 & 206 & -57336 & -28988 & -55202 & -101490 & -115129 & 229 & 460 & -32 & -4205 & \\ -736 & 589 & 309 & -2660 & 65119 & 32693 & -64326 & -323340 & 879 & 726 & 310 & -29587 & \\ 479 & -225 & 205 & -546 & -345 & 411 & 337 & 3900 & -982 & -473 & -202 & 153 & \\ 317 & -239 & 9 & 191 & -125 & 169 & 428 & 2060 & -446 & -588 & -116 & 95 & \\ 3 & -1 & 202 & 147 & 14 & 150 & 12 & -6 & 1 & -4 & -252 & 141 & \\ 22 & 0 & -39 & 54231 & 9989 & 54179 & 9697 & -412 & 3 & -19 & 269 & -22333 & \end{array}\right)$$

x_1: x position in local coordinate system of pulley, local coordinate system rotated 30 degrees counterclockwise around global y at t=0 s

x_2: z position in local coordinate system of cradle center of mass parallel with global z at t=0 s

x_3: z position in local coordinate system of left front foot parallel with global z at t=0 s

x_4: y position in local coordinate system of right front foot parallel with global y at t=0 s

x_5: z position in local coordinate system of right front foot parallel with global z at t=0 s

x_6: y position in local coordinate system of left rear foot parallel with global y at t=0 s

x_7: x position in local coordinate system of bottom housing plate center, parallel with global x at t=0 s

x_8: x position in local coordinate system of imbalance load, located at the front bottom of the drum, parallel with global x at t=0 s

x_9: x position in local coordinate system of top spring attachment plate center, parallel with global x at t=0 s

x_{10}: y position in local coordinate system of top spring attachment plate center, parallel with global y at t=0 s

x_{11}: y position in local coordinate system of top housing plate center, parallel with global y at t=0 s

x_{12}: y position in local coordinate system of rotating part of motor, parallel with global y at t=0 s

x_{13} to x_{24}: velocities of the above quantities.